

# Non-thermal Plasma Activates Human Keratinocytes by Stimulation of Antioxidant and Phase II Pathways

Received for publication, August 14, 2014, and in revised form, January 12, 2015. Published, JBC Papers in Press, January 14, 2015, DOI 10.1074/jbc.M114.603555

Anke Schmidt<sup>†S1</sup>, Stephan Dietrich<sup>‡</sup>, Anna Steuer<sup>S</sup>, Klaus-Dieter Weltmann<sup>S</sup>, Thomas von Woedtke<sup>S</sup>, Kai Masur<sup>‡2</sup>, and Kristian Wende<sup>‡2</sup>

From the <sup>†</sup>Centre for Innovation Competence (ZIK) plasmatis and <sup>S</sup>Leibniz Institute for Plasma Science and Technology, Felix-Hausdorff-Strasse 2, 17489 Greifswald, Germany

**Background:** Non-thermal plasma provides an interesting therapeutic opportunity to control redox-based processes, e.g. wound healing.

**Results:** The transcription factor NRF2 and downstream signaling molecules were found to act as key controllers orchestrating the cellular response.

**Conclusions:** Plasma triggers hormesis-like processes in keratinocytes.

**Significance:** These findings facilitate the understanding of plasma-tissue interaction and its deduced clinical application.

Non-thermal atmospheric pressure plasma provides a novel therapeutic opportunity to control redox-based processes, e.g. wound healing, cancer, and inflammatory diseases. By spatial and time-resolved delivery of reactive oxygen and nitrogen species, it allows stimulation or inhibition of cellular processes in biological systems. Our data show that both gene and protein expression is highly affected by non-thermal plasma. Nuclear factor erythroid-related factor 2 (NRF2) and phase II enzyme pathway components were found to act as key controllers orchestrating the cellular response in keratinocytes. Additionally, glutathione metabolism, which is a marker for NRF2-related signaling events, was affected. Among the most robustly increased genes and proteins, heme oxygenase 1, NADPH-quinone oxidoreductase 1, and growth factors were found. The roles of NRF2 targets, investigated by siRNA silencing, revealed that NRF2 acts as an important switch for sensing oxidative stress events. Moreover, the influence of non-thermal plasma on the NRF2 pathway prepares cells against exogenic noxae and increases their resilience against oxidative species. Via paracrine mechanisms, distant cells benefit from cell-cell communication. The finding that non-thermal plasma triggers hormesis-like processes in keratinocytes facilitates the understanding of plasma-tissue interaction and its clinical application.

Due to the recent advances in the development of non-thermal plasma sources operating at atmospheric pressure, the treatment of living cells and tissues with a mixture of plasma components has become possible (1). Non-thermal plasma was described to have antimicrobial activity and to play an important role in the killing of microorganisms (2–5). These developments resulted in a new and independent field, plasma medicine, in which one promising approach is to promote wound closure by stimulation of the cells involved. There are numer-

ous possibilities how plasma influences cells at a molecular and genetic level (6, 7). However, knowledge about cellular signaling events subsequent to plasma treatment of eukaryotic cells or tissues is still rudimentary. The molecular and cellular mechanisms of plasma-induced *in vitro* effects on keratinocytes have to be examined with particular emphasis on the roles of reactive oxygen (ROS)<sup>3</sup> and nitrogen species (RNS), growth factors, chemokines, and chemoattractants.

Keratinocytes as a cell culture model for wound healing (8) are a component of the primary skin layer and represent a major factor for tissue repair and regeneration. Under physiological conditions, ROS/RNS are produced in the skin continuously (9). Besides other cells, keratinocytes also express ROS-detoxifying enzymes and possess an inducible defense system (10, 11). It is a well known fact that ROS/RNS are cellular modulators and signaling molecules that play an integral part in immune responses, cell differentiation, and regulation of angiogenesis (12, 13). In addition, it was shown that keratinocytes play a crucial role in wound healing (14–17), regulation of several proteins of the coagulation cascade, and platelet recruitment and activation (18, 19).

Due to the fact that many healing processes are controlled by redox reactions, the application of non-thermal plasma provides an interesting therapeutic tool in redox-based wound healing. Such plasma contains variable compositions of ultraviolet light, free electrons, and charged particles as well as ROS (e.g. HO<sup>•</sup>, O<sub>2</sub><sup>-•</sup>, O<sub>3</sub>, and H<sub>2</sub>O<sub>2</sub>) and RNS (e.g. NO<sup>•</sup> and ONOO<sup>-</sup>) including bioactive substances (NO and H<sub>2</sub>O<sub>2</sub>) (20). A further

<sup>1</sup> To whom correspondence should be addressed: INP Greifswald, Dept. Plasma Bioengineering, Felix-Hausdorff-Strasse 2, 17489 Greifswald, Germany. Tel.: 49-03834-5543958; Fax: 49-03834-554301; E-mail: anke.schmidt@inp-greifswald.de.

<sup>2</sup> Both authors made equal contributions to this work.

<sup>3</sup> The abbreviations used are: ROS, reactive oxygen species; RNS, reactive nitrogen species; ARE, antioxidant-responsive element; NRF2, nuclear factor erythroid-related factor 2; KEAP1, Kelch-like ECH-associated protein 1; HMOX1, heme oxygenase 1; NQO1, NADPH-quinone oxidoreductase 1; qPCR, quantitative real time PCR; GCLC,  $\gamma$ -glutamylcysteine ligase catalytic subunit; GCLM,  $\gamma$ -glutamylcysteine ligase modifier subunit; SOD, superoxide dismutase; GPX, glutathione peroxidase; NHEK, normal human epidermal keratinocyte; IPA, Ingenuity Pathway Analysis; Panther, Protein Analysis through Evolutionary Relationships; AP-1, activator protein 1; CAT, catalase; HBEGF, heparin-binding EGF-like growth factor; TRX, thioredoxin; GSR, glutathione reductase; PPAR $\alpha$ , peroxisome proliferator-activated receptor  $\alpha$ ; MSP, macrophage-stimulating protein.

## Plasma Triggers Hormesis-like Processes in Keratinocytes

favorable advantage of non-thermal plasma is the generation of reactive species at the site of interest such as wounds or skin diseases where they can directly function as signaling molecules. In this context, the general applicability of cold plasmas to treat the skin or infected wounds *in vivo* has been investigated (21–26).

An imbalance between the production and detoxification of reactive intermediates affects the cellular stress level. For example, the redox balance influences the maintenance of cell proliferation rhythms like the cell cycle (12). Beyond that, changes in ROS levels trigger a coordinated action of transcription factors (27). The nuclear factor erythroid-related factor 2 (NRF2), a basic leucine zipper transcription factor, activates cellular rescue pathways against oxidative injury, inflammation, and apoptosis and activates downstream signaling. NRF2 plays a key role in regulation of genes that encode detoxifying enzymes and antioxidant proteins and functions in cellular defense against imbalances in redox homeostasis. Under basal conditions, NRF2 is associated with an actin-binding protein, Kelch-like ECH-associated protein 1 (KEAP1), which retains NRF2 in the cytoplasm where it is targeted for ubiquitin-mediated degradation (28). KEAP1, a vital factor in the NRF2 signaling cascade, is a protein containing Kelch-1-like and BTB/POZ domains (29). Small amounts of constitutively nuclearly localized NRF2 maintain cellular redox homeostasis through regulation of basal expression of antioxidant genes. After release of NRF2 from KEAP1 by oxidation events at cysteine, NRF2 translocates to the nucleus, binds to antioxidant-responsive elements (AREs) in the promoters of its target genes and activates their transcription (30). Such genes encode among others ROS-detoxifying enzymes and antioxidants and proteins such as glutathione *S*-transferase, cytochrome P450, NADPH-quinone oxidoreductase 1 (NQO1), heme oxygenase 1 (HMOX1),  $\gamma$ -glutamylcysteine ligase catalytic (GCLC) and modifier subunits (GCLM), superoxide dismutases 1–3 (SOD1–3), thioredoxin (TRX), catalase (CAT), glutathione peroxidase (GPX), and non-enzymatic antioxidants like glutathione. In addition, in the absence of oxidative stress in eukaryotes, the basic region leucine zipper transcriptional regulator BACH1 binds AREs and represses transcription (31, 32). BACH1 forms heterodimers with the basic leucine zipper subfamily of small MAF proper noun protein and binds the MAF recognition element in the promoter regions of HMOX1 and NQO1 (33). Although the role of BACH1 as a regulator of gene expression after plasma treatment is uncharacterized, it was previously shown that BACH1 antagonize NRF2-mediated induction of HMOX1 through its interaction with multiple ARE/activator protein 1 (AP-1) sites (34).

Previous data suggested that plasma induces cell reactions of stress sensing along increased expression of enzymes of the antioxidant defense system. The analysis further indicated that stimulating properties on keratinocytes make non-thermal plasma a promising option in treatment of wounds (7). Our present study used both a whole-genome microarray and a proteome approach to obtain insights into potential mechanisms of plasma activation in human keratinocytes. We used an atmospheric argon plasma jet kinpen (neoplas GmbH, Greifswald, Germany) to identify potential applications of non-thermal plasma to

accelerate wound healing processes. Hundreds of genes and proteins were identified that were significantly changed in at least one treatment group. Independent from treatment duration, we clarify some of the mechanisms of action in plasma-treated keratinocytes. In general, non-thermal plasma treatment clearly induced a strong antioxidant effect together with a plasma-related activation of the NRF2/KEAP1 pathway. Further analysis revealed increased expression of NRF2 downstream targets that play important roles for cell protection.

### EXPERIMENTAL PROCEDURES

**Cell Culture and Transfection**—HaCaT (human adult low calcium high temperature keratinocytes) cells were obtained from the German Center of Cancer Research (DKFZ, Heidelberg, Germany) and were cultured in Roswell Park Memorial Institute (RPMI) 1640 medium. The medium was supplemented with 10% fetal calf serum (FCS) (Sigma), 1% penicillin G/streptomycin (Lonza), and cells were cultured under 5% CO<sub>2</sub> at 37 °C. Primary keratinocytes (NHEK cells) were obtained from PromoCell GmbH (Heidelberg, Germany) and cultured in PromoCell medium. Transfection of HaCaT cells with appropriate siRNA was carried out when they were 50–60% confluent using X-tremeGENE siRNA transfection reagent (Roche Applied Science) according to the manufacturer's instructions.

**Measurement of Hydrogen Peroxide and ROS Production**—Hydrogen peroxide production in medium was measured fluorometrically using 1  $\mu$ M Amplex<sup>®</sup> Red (10-acetyl-3,7-dihydroxyphenoxazin) and 10 units/ml horseradish peroxidase. Cells were resuspended in the phosphate-buffered saline (PBS) and incubated with plasma-treated medium for 30 min at 37 °C. Reagents were added, and the rate of hydrogen peroxide production was quantitated at 560-nm excitation and 585-nm emission by a microplate fluorometer (Tecan F200, Gröding, Austria). Intracellular ROS production in HaCaT cells was determined utilizing 2',7'-dichlorofluorescein diacetate (Sigma). Briefly, 10<sup>6</sup> cells in a 6-cm culture dish were incubated with plasma-treated medium or H<sub>2</sub>O<sub>2</sub> (100  $\mu$ M) for the indicated times. Then the cells were collected and incubated with 10  $\mu$ M 2',7'-dichlorofluorescein diacetate for 30 min at 37 °C. Cells were centrifuged, and the pellets were washed twice with ice-cold PBS and resuspended in FACS buffer. Fluorescence intensity was measured by flow cytometry with an excitation wavelength of 488 nm and an emission wavelength of 530 nm.

**Exposure of Human Cells to Non-thermal Plasma**—Non-thermal plasma was produced using an atmospheric pressure argon plasma jet in air (kinpen). Several treatment times (20, 60, and 180 s) were chosen to clarify effects of treatment intensity on cellular changes after indirect plasma treatment. Plasma treatment was performed in an indirect treatment regimen using a motorized stage. "Indirect" means that only the liquid medium (5 ml of RPMI 1640 medium) came into direct contact with the plasma. Immediately after treatment, medium was transferred to a dish containing one million HaCaT, 293, or NHEK cells, allowing generated ROS/RNS to interact with the cells (7). This procedure has been found to have effects on the cells comparable with treatment of the medium when covering the cells directly (35). 2 h after plasma exposure, fresh medium was added, and cells were incubated for a further 1, 4, and 22 h

before collection, centrifugation, and washing. Cells treated with 100  $\mu\text{M}$   $\text{H}_2\text{O}_2$  served as positive controls for oxidative stress corresponding to the above described plasma treatment equivalents. To exclude effects of the carrier gas, cells treated with argon gas were used as negative controls. Subsequently, all control samples and plasma-treated and untreated cells were analyzed and compared with respect to their gene activity. For the proteome approach, complete RPMI 1640 medium was treated in triplicates for 180 s in the same manner as described above. Medium was transferred immediately into dishes containing cells and kept in an incubator for 3, 6, or 24 h. Control cells were not plasma-treated but otherwise treated identically (Fig. 1).

**Analysis of Cell Viability and Programmed Cell Death**—Cells were seeded in 6-well plates, and after 24 h of cell attachment, the cells were exposed to plasma-treated medium as indicated. The viability of HaCaT cells was assessed by a dye-based method: calcein (*green*)/propidium iodide (*red*) staining for living and dead cells, respectively. Apoptotic cells were detected by terminal deoxynucleotidyltransferase-mediated dUTP-biotin nick end labeling (TUNEL) stain. The cells were fixed and permeabilized using a mixture containing 0.1% Triton X-100 in PBS followed by treatment with the Click-iT<sup>®</sup> TUNEL Alexa Fluor<sup>®</sup> 594 imaging assay (Invitrogen) at 37 °C for 60 min. The apoptotic cells (pink) were visualized using fluorescence microscopy (Zeiss AG, Oberkochen, Germany).

**Sample Preparation for Gene Expression Profiling**—Total RNAs from each group were purified and isolated using an RNA mini kit (Biosell, Germany), and RNA integrity was confirmed using the 2010 Bioanalyzer (Agilent) as described (7). Briefly, cDNA was synthesized from 10  $\mu\text{g}$  of total RNA using a cDNA synthesis kit (Life Technologies) in the presence of oligo(dT) primer (200 ng/ml). Double strand cDNAs were labeled with fluorescent Cy3 dye. A global gene expression study was carried out using multiplex arrays containing a fourplex format ( $4 \times 72,000$ ) with 24,000 different human-specific probes per array ( $n \geq 3$ ). Hybridization and washing of gene chips were done according to the supplier's instruction, and slides were analyzed by a Microarray Laser Scanner (MS 200). If not otherwise stated, all kits, microarrays, and software programs were provided by Roche NimbleGen (Mannheim, Germany).

**Gene Expression Data Acquisition and Processing**—Signal intensity values were translated into gene ID lists including expression values using DEVA1.1 software. Background-corrected signal intensities were determined and processed using robust multichip averaging analysis (36). Quantile normalization of microarray data, statistical tests, and further filtering methods were accomplished by analysis software. Data handling and all calculations including cluster analysis were performed using Partek Genomic Suite. To find the differentially expressed genes, expression data were grouped according to treatment conditions and statistically analyzed using multiple testing corrections (37). The gene ontology terms were determined by uploading the gene list on the Protein Analysis through Evolutionary Relationships (Panther) classification system. Gene family classification from Panther represents various gene families that are over- or underrepresented for all scenarios. Ingenuity Pathway Analysis (IPA) was applied to summarize the effect of gene expression changes and to obtain

top biological functions, pathways, and networks associated with plasma treatment.

**Protein Separation and Digestion**—Total cellular protein was harvested by lysis using radioimmune precipitation assay buffer (1% Igepal CA-630, 0.5% sodium deoxycholate, 0.1% sodium dodecyl sulfate, 2 mM EDTA, Roche Applied Science cOmplete protease inhibitor mixture, 2 mM phenylmethanesulfonyl fluoride). After clearance by centrifugation ( $10,000 \times g$  at 4 °C), the supernatant was used for further analysis. Proteins were fractionated by SDS gel electrophoresis (ProGel Tris glycerin 10%) for 120 min at 125 V in electrophoresis buffer (20 mM Tris, 200 mM glycine, 3.5 mM SDS, pH 8.3). After washing ( $2 \times 2$  min with Millipore water) and fixation for 20 min in methanol/water/acetic acid (50:40:10), the gel was cut into lanes with 12 fractions each. In-gel protein digestion was performed using sequencing grade trypsin at 1:50 (Promega, Mannheim, Germany) overnight at 37 °C. After peptide extraction from the gel pieces using a step gradient of formic acid/acetonitrile and concentration/acetonitrile removal (aqueous settings, SpeedVac Concentrator, Eppendorf, Hamburg, Germany), the peptide mixture was subjected to liquid chromatography/mass spectrometry (LC/MS).

**Liquid Chromatography and High Resolution Mass Spectrometry**—The peptide mixture was analyzed by nano-LC/MS. Briefly, peptides were separated on a 30-cm/75- $\mu\text{m}$ -inner diameter fused silica column (Aeris, 3  $\mu\text{m}$ , RP18, Phenomenex, Aschaffenburg, Germany) using a Proxeon nanoLC II (Thermo Fisher Scientific) and a water, 0.1% acetic acid/acetonitrile, 0.1% acetic acid gradient (0.3  $\mu\text{l}/\text{min}/120$  min). Eluent was ionized by an electrospray ionization technique (NanoSpray III source), and ions were analyzed using an ABSciex TripleTOF 5600 mass spectrometer. All samples were injected twice. Raw data were then analyzed for peptide and protein identification using ProteinPilot 4.5 software (Paragon algorithm). Identified proteins were relatively quantified using PeakView, a protein quantitation tool. After normalization in MarkerView, further data processing to obtain information on the protein expression pattern and statistical analysis were done using Partek, the Panther database, and IPA.

**Gene Validation Using Quantitative Real Time PCR**—To confirm changes in the expression of selected genes, RNA samples from each treatment group including those analyzed by microarray were assayed by quantitative real time RT-PCR. Quantitative real time RT-PCR was performed on a 96-well LightCycler 480 qPCR system (Roche Diagnostics Ltd.) according to the manufacturer's protocols. For quantification of several mRNAs by qPCR, 1  $\mu\text{g}$  of RNA was transcribed into cDNA as described previously (7). Using SYBR Green I Master (Roche Diagnostics Ltd.), quantitative real time RT-PCR was conducted using 20 ng of cDNA in triplicate with internal and no-template controls. Primer sequences of target genes *NRF2*, *KEAP1*, *NQO1*, *HMOX1*, *SOD*, *CAT*, *VEGFA*, *HBEGF*, *GCLC*, *GCLM*, and *GSR* were purchased from Roche Diagnostics Ltd. The protocol included preincubation at 95 °C for 3 min, 45 cycles of 95 °C for 10 s, annealing for 20 s at 55 °C, and amplification for 1 s at 72 °C. A SYBR Green detection reporter system was used, and the reactions generated a melting temperature dissociation curve enabling quantitation of the PCR products. The housekeeping gene *RPL13A*, whose expression was unaf-

## Plasma Triggers Hormesis-like Processes in Keratinocytes

ected by plasma, was used as an internal control for normalization in parallel with each gene of interest. To verify reproducibility, each sample was analyzed in triplicate in three independent experiments for each gene. The expression of the single genes was analyzed using the  $\Delta\Delta\text{CT}$  method. The final value for gene expression in each plasma-treated sample was determined as a ratio of the gene expression in the respective sample related to the control.

**Western Blot Analysis**—HaCaT cells were incubated with cell culture medium treated under the same condition as described above. Following incubation for a distinct time at 37 °C, cells were rinsed once with ice-cold PBS, spun down, and lysed in ice-cold lysis buffer/radioimmune precipitation assay buffer containing protease and phosphatase inhibitors (cOmplete Mini and phosSTOP; Roche Applied Science) and freshly added 2 mM phenylmethanesulfonyl fluoride (PMSF; Carl Roth, Karlsruhe, Germany). Subsequently, cells were ultrasonicated (Labsonic M Ultrasonicator, Sartorius) by applying two pulses at 50% of nominal power with a duty cycle of 50 and kept on ice for 30 min. Lysates were centrifuged at 10,000  $\times g$ . Supernatants were isolated, and protein concentration was adjusted in all samples prior to heating to 95 °C for 5 min in 5 $\times$  sample buffer (1.25 M Tris, 10% SDS, 50% glycerol, 10%  $\beta$ -mercaptoethanol, 0.02% bromophenol blue) and subjected to sodium dodecyl sulfate-polyacrylamide gel electrophoresis (SDS-PAGE) on precast 10% PAGE gels (Abcam, Cambridge, UK). Proteins were blotted onto Roti<sup>®</sup> PVDF membranes (Carl Roth). Subsequently, unspecific binding was blocked with 3% bovine serum albumin (BSA; Carl Roth) in Tris-buffered saline (20 mM Tris, 13.7 mM NaCl) containing 0.1% Tween (TBST) for 30 min. After this, the membrane was incubated with the corresponding primary antibody at 1:200 at 4 °C overnight. Antibodies against NRF2 (sc-13032), HMOX1 (sc-1796), NQO1 (sc-6464), and KEAP1 (sc-15246) were obtained from Santa Cruz Biotechnology (Heidelberg, Germany). Incubation was followed by three washing steps with TBST and incubation with horseradish peroxidase-coupled secondary antibodies at 1:10,000 for 1 h at room temperature. After three washing steps in TBST, membranes were incubated with Serva Light Polaris (Serva Electrophoresis GmbH, Heidelberg, Germany) and imaged using the ImageQuantLAS4000 (GE Healthcare). The same membranes were stripped and reprobated with antibodies directed against  $\beta$ -actin (sc-9104) as a loading control. Band intensities were quantified using ImageQuantTL software (GE Healthcare), normalized to actin, and expressed as the percentage of -fold change compared with the corresponding control.

**Immunofluorescence Microscopy**—HaCaT, NHEK, and 293 cells were grown on glass coverslips in 6-well plates. Cells were transfected with siRNA for NRF2, KEAP1, or BACH1. 72 h after transfection, cells were incubated with plasma-treated medium for 20 min, washed twice with PBS, and fixed with 4% (w/v) paraformaldehyde for 20 min at room temperature. Cells were permeabilized with PBS, 0.2% Triton X-100 for another 20 min and blocked with PBS, 1% BSA. Slides were washed twice with PBS, 1% BSA and incubated at 4 °C for 24 h with primary NRF2 antibody at a 1:200 dilution in PBS. Actin cytoskeleton was stained with phalloidin-FITC. Afterward, cells were washed twice in PBS and incubated with secondary Alexa Fluor 546-

conjugated goat anti-rabbit antibody (1:700; Life Technologies) for 1 h. Coverslips were washed again in PBS and mounted onto glass microscope slides using Vectashield<sup>®</sup> HardSet<sup>™</sup> mounting medium. Images were obtained using an Axio Observer Z1 (Zeiss AG).

**Enzyme Activity Assay**—Cellular NQO1 (P15559) activity was obtained by measuring the menadione reduction in the presence or absence of the NQO1 inhibitor dicoumarol using a commercially available kit (Abcam). The protocol suggested by the supplier was followed except that extraction buffer was supplemented by protease inhibitors (1 mM PMSF). Cells were treated as described above and lysed 6 or 24 h after treatment. 50  $\mu\text{l}$  of lysate was assayed. Human GPX activity was determined indirectly by the quantification of the enzymatic creation of glutathione disulfide under the effects of cumene hydroperoxide and its reduction by glutathione reductase using a commercially available kit (Cayman Chemical Co., Ann Arbor, MI). The protocol suggested by the supplier was followed, and samples were used undiluted (20  $\mu\text{l}$ ). Cells were prepared as described above, and cell lysate was obtained 3, 6, and 24 h after treatment by scraping on ice using a 50 mM Tris buffer, pH 7.5 supplemented with 5 mM EDTA and 1 mM dithiothreitol. Protein contents were determined using the Bio-Rad RC DC assay and an appropriate standard curve prepared in extraction buffer.

**Statistical Analysis**—Statistical significance was estimated by two-way analysis of variance followed by a calculation of means and S.D. Student's *t* test was used to determine the degree of statistical significance between values from different experimental groups. Each experiment was performed at least three times. The threshold was set to 3-fold, and the difference was considered statistically significant when  $p \leq 0.05$  (>3-fold change). All statistical analyses were performed using GraphPad Prism 6, Partek, and Ingenuity Pathway Analysis. Statistical analysis to evaluate the effects of siRNA on gene expression was carried out using on-way analysis of variance.

## RESULTS

**ROS Generation, Cell Viability, and Apoptosis Assays after Plasma Treatment**—In addition to various molecular sources including NADPH oxidase and mitochondrial electron leakage that may contribute to ROS formation in response to oxidative stress (38), the role of plasma as a trigger of oxidative stress level alterations has not been extensively investigated. Plasma-generated reactive species were assigned to act a major part of plasma effects and add to the cellular production level of endogenous ROS/RNS (39, 40) (Fig. 1). Consequently, the study investigated the plasma-induced ROS formation in the plasma-treated medium and in HaCaT cells. As illustrated in Fig. 2, plasma treatment has a significant impact on ROS levels, in particular on H<sub>2</sub>O<sub>2</sub> formation: we obtained a treatment time-dependent generation of H<sub>2</sub>O<sub>2</sub> from 15 (20 s) to 32  $\mu\text{M}$  (60 s) and 100  $\mu\text{M}$  (180 s) in the plasma-treated medium, respectively (Fig. 2A). To assess changes in the intracellular ROS levels, 2',7'-dichlorofluorescein diacetate conversion was quantified by flow cytometry. 30 min after plasma exposure to medium, the ROS level was approximately 2 times higher in short term plasma-treated cells (20 s) and 4 times higher in long term plas-

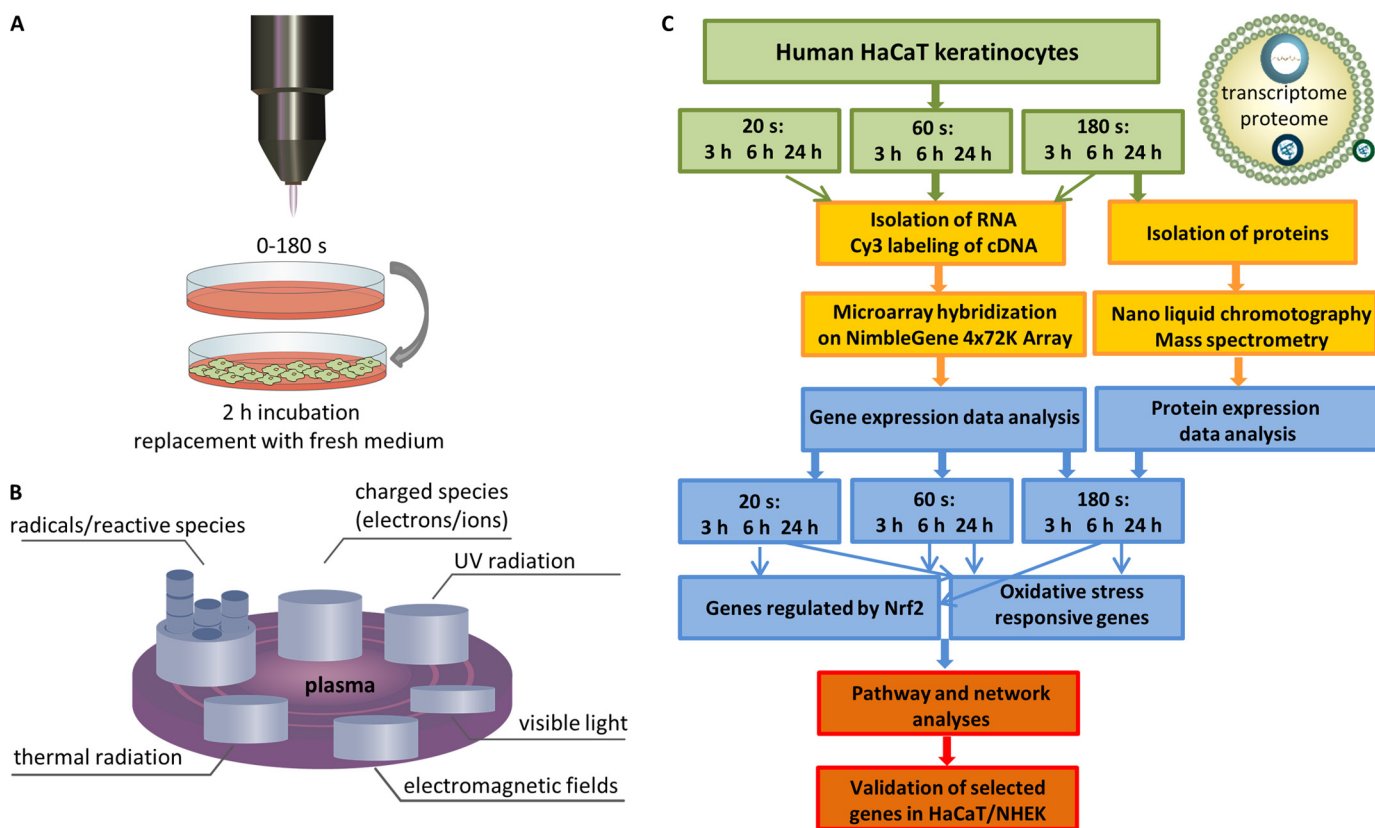


**FIGURE 1. Schematic setup of the plasma treatment using kinpen and sample preparation for gene and protein expression profiling.** *A* and *B*, the kinpen source produces a jet-type plasma with an effluent containing a variable mixture of active components: reactive molecules, radicals, electrons, ions, and different types of radiation (electric fields and thermal and ultraviolet radiation). *C*, for assessment of transcriptome and proteome changes, cell culture medium was plasma-treated for the lengths of time indicated and applied to the HaCaT keratinocyte cell culture. The central element of the whole experimental procedure is the transcriptome analysis using microarrays containing  $4 \times 72,000$  gene data sets. Data analysis using Partek Genomic Suite, Panther database, and Ingenuity Pathway Analysis summarizes gene expression levels of each transcript and allows conclusions on cell physiology under the following conditions: 0, 20, 60, and 180-s treatment of cell culture medium including 2-h incubation of HaCaT cells. Afterward, cells were incubated with fresh medium for 1, 4, and 22 h. Liquid chromatography and mass spectrometry were performed for the 180-s treatment group.

ma-treated cells (180 s) compared with the untreated controls. Similar results were obtained when ROS production was measured after 60-min incubation. 180 s of plasma treatment led to ROS generation comparable to that of  $\text{H}_2\text{O}_2$  treatment ( $100 \mu\text{M}$ ), whereas shorter treatment times show a significant lower ROS formation level (Fig. 2*B*).

In addition, cell viability measurements were used to monitor the vitality of cells after plasma treatment (Fig. 2*C*). Even after longer exposure to plasma, we detected a survival rate of more than 90% of cells. A TUNEL assay confirmed low cytotoxic and apoptotic effects in HaCaT cells. The treatment regime chosen excludes a significant role of apoptosis after plasma exposure. At the highest plasma treatment time, we only found a marginal increase of the number of TUNEL-positive cells up to 10% (Fig. 2*D*).

**Gene Expression Profiling in HaCaT Cells and Functional Enrichment Analysis**—Furthermore, all plasma samples were analyzed and compared with respect to their gene activity. The data of gene expression profiling have been uploaded to the NCBI Gene Expression Omnibus under accession number GSE58395. Evaluation of the data using Partek Genomic Suite allowed the identification of regulated genes according to non-thermal plasma features. Gene expression data of both increased and decreased gene groups were determined to

identify regulated genes represented by several experimental groups. Our findings demonstrate that a large number of genes are differentially expressed after incubation with plasma-treated medium. All transcripts were clustered into two distinct expression patterns following a hierarchical clustering of similarity (data not shown).

Aiming at evaluating the genes, pathways, and biological processes involved in the observed response against plasma, several treatment times (20, 60, and 180 s) were chosen to clarify effects of treatment intensity on cellular changes after indirect plasma treatment. Moreover, a comparison among 3-h, 6-h, 24-h, and control groups was carried out. If not indicated otherwise, all experimental groups were named according to their incubation time (e.g. 3-h group) or to their treatment time (e.g. 20-s group). Venn diagrams were constructed to identify common and exclusively up- or down-regulated genes corresponding to sampling time. After 3 h, we obtained total data for  $\sim 1,200/560/400$  differentially expressed genes for each treatment time (3-fold change,  $p \leq 0.05$ ; Fig. 3*A*). The number of modulated genes increased to 2,100/2,350/5,000 genes after 6 h (identified as statistically significant in the study; Fig. 3*A*). After 24 h, we found a total number of 300/120/700 regulated genes, respectively (Fig. 3*A*). Venn diagrams also visualize the overlapping results between the differentially regulated genes found at 3

## Plasma Triggers Hormesis-like Processes in Keratinocytes

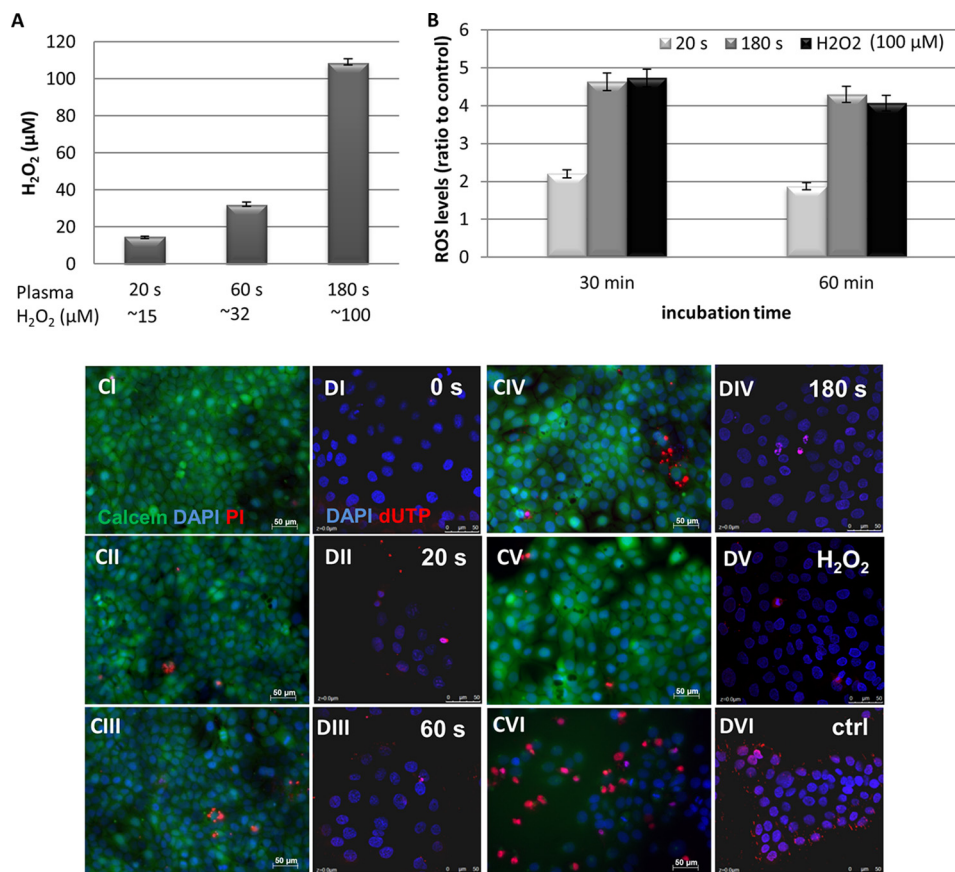


**FIGURE 2. Assessment of hydrogen peroxide and ROS production as well as cell viability and DNA fragmentation in HaCaT cells.** *A*, cells were incubated with plasma-treated medium for the length of time indicated, and generation of H<sub>2</sub>O<sub>2</sub> was measured using an Amplex Red assay ( $n = 3$ ). After 20, 60, and 180 s, approximately 15, 32, and 100 μM H<sub>2</sub>O<sub>2</sub> was generated in plasma-treated medium. *B*, ROS levels were quantified after short (20-s) and long term (180-s) plasma treatment following 30- or 60-min incubation of cells with plasma-treated medium. H<sub>2</sub>O<sub>2</sub> (100 μM) exposure of HaCaT cells shows the same ROS level as long term treatment. Error bars represent S.D. *CI–CVI*, cell viability measured by a calcein/propidium iodide (PI) assay in HaCaT cells exposed to increasing plasma treatment times. Representative images of randomly selected microscopy images of HaCaT cells stained with calcein/propidium iodide after plasma exposure show no dose-dependent cytotoxic effect in plasma-treated groups: there was not a strong decrease in viability at higher concentrations ranging from 0 to 180 s (low or no green fluorescence; red fluorescence indicates cell death). *DI–DVI*, apoptosis was assessed using the TUNEL assay. Representative microscopy images of TUNEL-positive apoptotic HaCaT cells (red) and counterstaining with Hoechst (blue) are shown. Cells exhibiting pink fluorescence are positive for both dead cells and nuclei. TUNEL analysis revealed that the number of apoptotic cells in plasma-treated cells was marginally higher than in untreated or short term plasma-treated cells. Scale bars, 50 μm. *ctrl*, control.

(150 genes for all experimental groups), 6 (900 genes), and 24 h (10 genes) versus control comparison (red numbers). In addition, we constructed Venn diagrams for each treatment time group (*i.e.* 20, 60, and 180 s) to show the distribution of genes within the treatment time groups (Fig. 3, *B–BII*). The highest numbers of differentially expressed genes were detected for the 6-h group and after long term plasma treatment. Yellow circles depict the total number of all differentially expressed genes within the indicated times.

After identifying the profiles of differentially expressed genes, we carried out functional enrichment analysis to reveal transcripts putatively involved in signaling pathways (41). Following statistical testing procedures, removal of the transcripts with no Entrez Gene ID, and -fold change cutoff (genes with -fold change  $\geq 3$ ), we found between 27 and ~2,500 regulated genes due to plasma treatment. The biology-focused pathway Panther classification system was used to better understand the significance of the differentially expressed genes in relation to each other and to identify the signaling cascades involved. Over- and underrepresented families were detected by comparison with untreated control. From all differentially expressed

transcripts, about 80% were found to have an annotation in the database. Based on gene ontology classification, the altered genes were functionally enriched (Fig. 4). Placement of genes into “molecular functions” finds genes, among others, that were strongly associated with transcriptional functions (*e.g.* transcription factors as the most overrepresented gene family; data not shown), nucleic acid binding, and signaling molecules (Fig. 4A). One relevant category represented in “molecular function class” was that of enzymes for regulation of antioxidant activity, *e.g.* oxidoreductases (data not shown). To identify biological processes that could discriminate plasma-treated from non-treated clusters, we classified genes into 11 categories according to their functional role in “biological processes” (Fig. 4B): *e.g.* modulated genes from each group were mainly related to metabolic (42–48%) and cellular (33–34%) processes, whereas genes belonging to “biological adhesion” (6%), “cellular organization” (5–7%), and “apoptosis” (3%) were less regulated following plasma treatment.

*Pathway Analysis Reveals the Main Biological Functions Modulated by Non-thermal Plasma*—IPA was performed to compare expression measurement as well as for an interpreta-

## Plasma Triggers Hormesis-like Processes in Keratinocytes

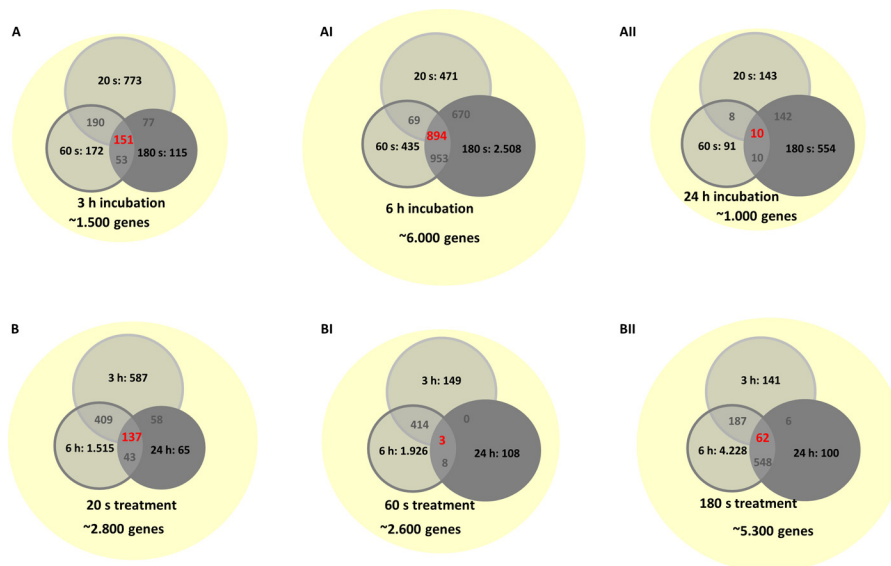


FIGURE 3. **Venn diagrams for regulated genes for each experimental group.** A–All, about 1,500 genes (3-h incubation), 6,000 genes (6 h), and 1,000 genes (24 h) were detected (*largest circles*). The indicated number of genes was found under either plasma condition or incubation time tested. Expression of genes (*number in the center of each*) was exclusively affected in all experimental groups by plasma. B–BII, Venn diagrams for 20-, 60-, and 180-s treatment groups. *Diameters of circles are to scale.*

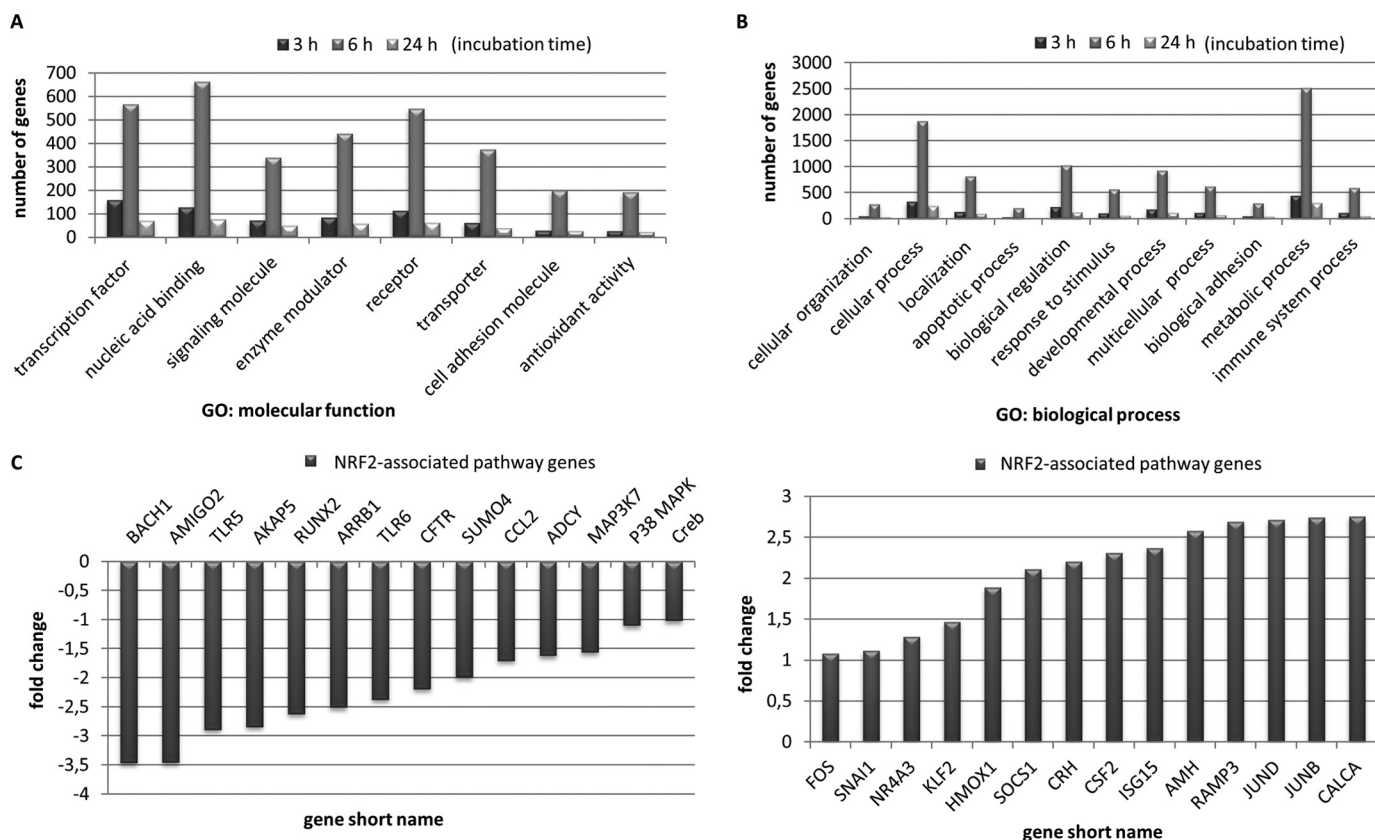
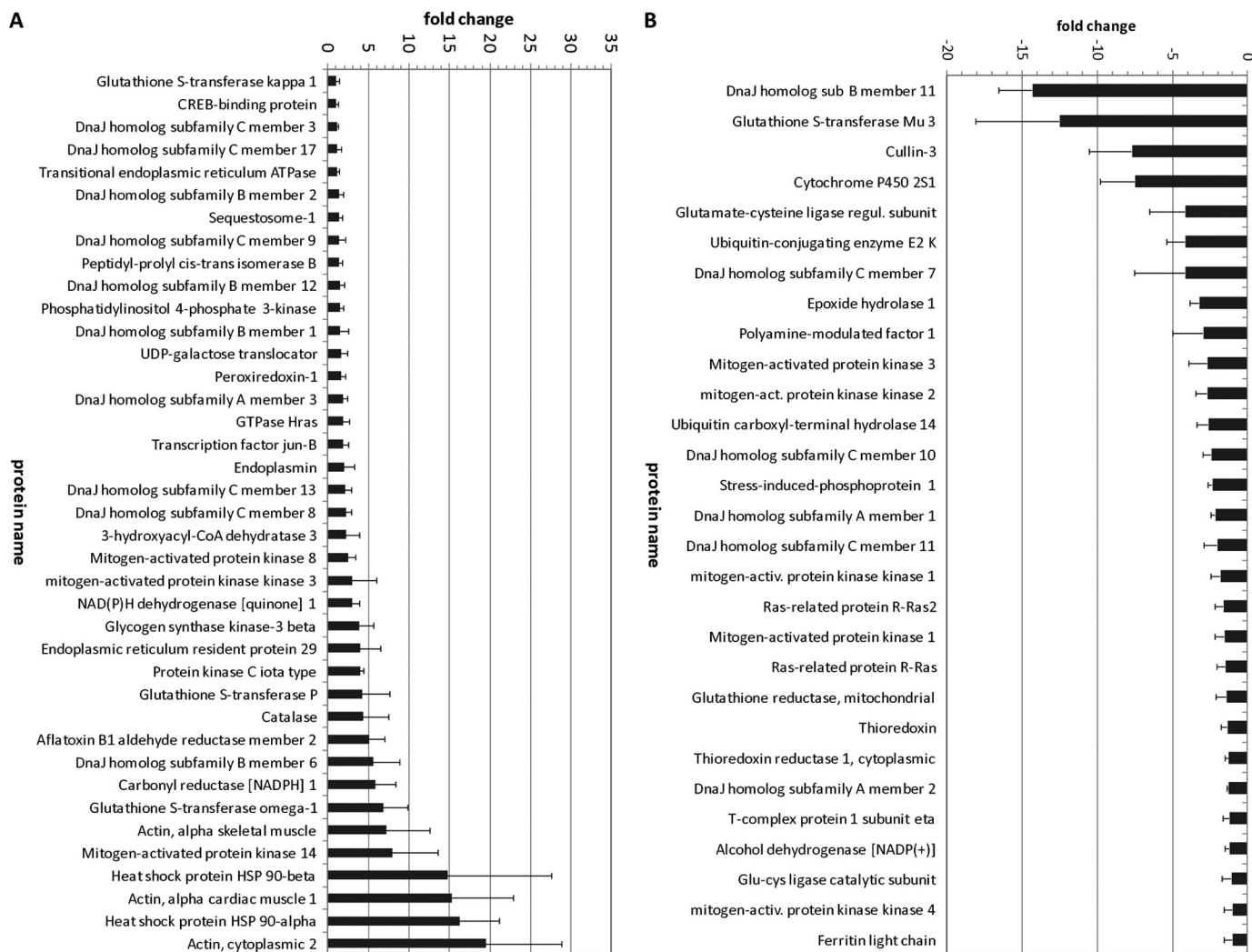


FIGURE 4. **Global gene expression in functional categories and protein classes using Panther software.** A and B, diagrams of microarray results (representing the number of differentially expressed genes) revealed similarities and differences in all transcriptome profiles found for 20, 60, and 180 s of plasma treatment. The open access Panther program was used to analyze the gene lists for each experimental group (analysis of 1,500, 6,000, and 1,000 sequences after 3-, 6-, and 24-h incubation, respectively) to find all categories with the “molecular function” (*left*) and “biological process” (*right*) function domain of gene ontology (GO) ( $p \leq 0.05$ ). *Bars* represent the number of genes with both enhanced and decreased expression. C, NRF2-associated pathway genes were identified in a gene expression microarray analysis: *left*, down-regulation; *right*, up-regulation.

tion of differential gene and protein expression on a molecular level. Our study evaluated how oxidative stress induced by plasma exposure leads to activation of several upstream factors. To high-

light this aspect, an important switch to control stress events is the activation of nuclear transcription factors. IPA annotation revealed that cellular reaction to plasma involved a considerable

## Plasma Triggers Hormesis-like Processes in Keratinocytes



**FIGURE 5. NRF2-related protein expression by human keratinocytes after plasma treatment according to IPA data reduction.** Cellular proteins were identified/quantified by liquid chromatography and high resolution mass spectrometry (180-s treatment, 8-h incubation; see “Experimental Procedures”). *A*, IPA revealed 40 proteins related to NRF2 signaling to be up-regulated (of which 23 proteins were up-regulated >2-fold), indicating the presence of oxidative stress. Among the up-regulated proteins, enzymes like NQO1 and carbonyl reductase 1 (*CBR1*) stand out. *B*, 29 proteins related to NRF2 signaling were down-regulated (or which 16 proteins were down-regulated >-2-fold). Glutathione S-transferases show a complex pattern with up- or down-regulation of different types, e.g. GSTO1 and GSTM3. Bars represent the mean of five data points  $\pm$  S.D. (error bars).

number of genes of the NRF2-mediated oxidative stress response pathway. This NRF2 signaling was ranked among the most active regulatory networks mainly in the 3-h groups. Up-regulated (Fig. 4C, right; e.g. *HMOX1*, *AMH*, *JUNB/D*, and *CSF2*) and down-regulated molecule targets (Fig. 4C, left; e.g. *BACH1*, *AMIGO2*, and *CFTR*) were identified and summarized as average expression-fold change in contrast to untreated control.

In a global proteome approach, we confirmed many of the differentially expressed genes. A total of 3,819 proteins were detected in all HaCaT lysates. About 400 of them were up-regulated more than 2-fold by the plasma treatment, whereas 350 proteins were down-regulated (>2-fold) (42). As expected, IPA predicted an increased oxidative stress on the basis of the detection and regulation of several proteins that act as sensors and/or effectors for this condition. Among these, the peroxiredoxins 1–6 and catalase were noticeable. In correlation to protein expression results, several ROS-scavenging enzymes like *GPX1*, -3, and -5; glutathione reductase; and peroxiredoxins displayed enhanced mRNA expression (7). The strongly increased abun-

dance of heat shock proteins (HSP90 and HSP40 derivatives) also indicates thermal or chemical stress. Proteins involved in thiol group reduction or coupling (*GSTK1*, *GSTO1*, and *GSTP1*) showed an increased abundance within the investigated time line. Thus, glutathione metabolism, which is a marker for the NRF2-related signaling events, was affected (NF2L2; 69 molecules; IPA *p* value,  $3.5 \times 10^{-8}$ ). Among the most robustly increased proteins, NQO1 and carbonyl reductase 1 were found (Fig. 5). However, some major downstream proteins could not be detected by LC/MS; e.g. *HMOX1* could not be detected, whereas *HMOX2* was found.

Moreover, response to stress by activation of those factors culminates in enhanced protein synthesis and transcriptional activity. Briefly, the transcription factors *FOS* and *JUNB/D* were detected in the microarray as differentially expressed (Table 1); both are components of the AP-1 complex. Furthermore, we obtained a plasma-induced altered expression of genes and proteins that are associated with mitogen-activated protein kinase (MAPK) signaling. Many of the downstream fac-

**TABLE 1**  
Gene expression changes (-fold change versus control) of components of AP-1 (JUN pathway) for the action of plasma in HaCaT cells  
ND, not detected.

Genes	Treatment time	Incubation time		
		3 h	6 h	24 h
FOS	20 <sup>s</sup>	1.23	2.13	ND
	60	1.39	1.69	ND
	180	3.94	2.64	ND
JUNB	20	3.63	4.03	1.73
	60	1.8	1.56	3.72
	180	4.15	4.29	1.85
JUND	20	4	4.12	ND
	60	1.9	2.12	ND
	180	5.54	4.03	ND

**TABLE 2**  
IPA annotation of the top pathways altered by plasma for each incubation time (3-, 6-, and 24-h groups) in HaCaT cells

Group	Pathway	p value	Ratio	Molecules
3 h	NRF2-mediated oxidative stress response	7.31E-02	12/144 (0.105)	AKR7L, Bach1, CYP2C19, FOS, HMOX1, JUNB/D, MAF, MAFK, MAP3K7, MAPK1, PIK3C2G
	p38 MAPK signaling	8.02E-02	8/76 (0.105)	DUSP1, HIST2H3C, IL1RAPL1/2, MAP3K7, MEF2C, PLA2G2E, TIFA
	PKC signaling	6.95E-03	10/92 (0.109)	CAMK2B/D, CFOS, FYN, HLA-DRB5, MAP3K7/13, MAPK1, NFATC3, PIK3C2G
	IL10 signaling	1.42E-02	7/54 (0.13)	FOS, HMOX1, IL1RAAPI1/2, MAP3K7, MAPK1, SOC3
	JAK/STAT signaling	9.18E-02	6/56 (0.107)	FOS, MAPK1, PIK3C2G, SOCS1/3/5
	GM-CSF signaling	9.18E-02	6/57 (0.105)	CAMK2B/D, CSF2, CSF2RA, MAPK1, PIK3C2G
6 h	MSP-RON signaling pathway	7.8E-03	14/32 (0.438)	ACTA1/2, ATM, CCI2, CSF1, CSF2RB, IL3RA, JAK2, KLK3, PIK3C2G, PIK3R1/3, TLR2/4
	3-Phosphoinositide biosynthesis	7.65E-03	21/67 (0.313)	ASP5, ATM, CDC25C, DUSP1/8, PIK3C2G, PIK3R1/3, PIP5K1B, PAPDC2, PPP1R16/1B, PTEN, PTPN20A/B, PTPRJ, PTPRN, SIRPA, SOC3, TPTE2
	TGF-β signaling	6.25E-02	25/75 (0.333)	ACVR1B, ACVR2A, AMH, BCL2, BMPR2, CDC42, GSC, HNF4A, INHA, JUN, MAPK1, MAPK3, MAPK14, NKX2-5, NODAL, RNF111, RUNX2, SMAD1, SMAD2, SMAD3, SMAD6, SOS2, TGFBR1, ZFYVE9, ZNF423
24 h	Neuronal NOS signaling	1.07E-04	4/12 (0.333)	CAMK2, CHRNA1, NOS1, RYR2
	γ-Glutamyl cycle	1.44E-03	3/6 (0.5)	GGT1, GGTL1/2
	MSP-RON pathway	8.48E-03	5/32 (0.156)	CSF1, CSF2RB, PIK3C2G, TLR2/4

**TABLE 3**  
IPA annotation of the top molecular and cellular functions for the action of plasma in HaCaT cells

Group	Molecular/cellular functions	Ratio	No.	Molecules
3 h	Nucleic acid metabolism	8.93E-04–3.27E-02	13	AKAP5, CALCA, CRH, GHRH, GHRHR, GLP1R, GLP2R, HMOX1, HTR1A, HTRIB, MRAP, NPCC, RAMP3, TSHR
	Small molecule biochemistry	8.93E-04–4.79E-02	17	AKAP5, CALCA, CRH, GHRH, GHRHR, GLP1R, GLP2R, GRM1/5, HMOX1, HTR1A, HTRIB, MRAP, NPCC, RAMP3, TSHR, TSPO, UROCI
	Cell signaling	3.01E-03–3.27E-02	25	AKAP5, CALCA, CRH, GHRH, GHRHR, GLP1R, HTR1A, HTRIB, KCNH2, MRAP, RAMP3, TSHR
	Cellular growth and proliferation	7.86E-03–1.07E-02	16	AMH, CCL2, CRH, FGFR1, FCER1A, FOS, GHRH, GHRHR, HMOX1, IGFBP5, MAPK1, Nr4A1/3, PPARα, RUNX2, TCF4
	Cellular development	8.4E-03–1.07E-02	15	AMH, CCL2, CRH, FGFR1, FCER1A, FOS, GHRH, GHRHR, HMOX1, IGFBP5, MAPK1, NR4A1/3, PPARα, TCF4
6 h	Nucleic acid metabolism	1.24E-04–4.13E-02	53	ABCA1, AKAP5, AQP1, CALCA, CRH, CRHR1, CRMP1, CYP3A4, DRD1-4, EIF2AK3, GCG, GLP1R, GPBAR1, HMOX1, HTR1A/B, MTNR1A, NME2, NPY, POMC, PTGER2/3, PTH1R, RAMP1-3, TBXA2R, TSHR
	Small molecule biochemistry	1.24E-04–3.71E-02	64	ABCA1, ADCY5, ADM2, AKAP5, CALCA, CRH, CRHR1, DRD1/2/4, GCG, GHRH, GHRHR, GLP1R, GLP2R, GPBAR1, GPR12, HTR1A, HTRIB, MRGPRD, NME2, NPY, OXER1, POMC, PTGER2, PTGER3, PTH1R, RAMP1, RAMP2, RAMP3, TAARI, TBXA2R, TSHR, ...
	Cell signaling	1.18E-03–2.68E-02	58	ABCA1, AKAP5, CALCA, CRH, CRHR1, DRD1/2/4, GCG, GHRH, GHRHR, GLP1R, GPBAR1, HTRIB, NME2, NPY, POMC, PTGER3, PTH1R, RAMP1-3, TBXA2R, TSHR
	Cell-to-cell signaling and interaction	4.13E-03–2.68E-02	10	CNR1, CRH, CRHR1, PSIP1, TGM2, TLR2-5
	Amino acid metabolism	7.37E-03–3.71E-02	9	DAO, DDC, GAD1, HDC, HNF4A, SDS, TAT, UROCI
24 h	Cellular development	1.66E-03–4.31E-02	19	BAX, CACNA1G, CSF2RB, CTGF, FUT4, FST, IL6, ITGB1, PCYT1B, PRKCA, PTGS2, RYR2, S1PR1/3, SLURP1, TCF4, TLR2/4
	Cellular growth and proliferation	1.66E-03–4.31E-02	16	BAX, CACNA1G, CSF2RB, CTGF, FUT4, FST, IL6, ITGB1, PCYT1B, PRKCA, PTGS2, RYR2, S1PR1/3, SLURP1, TCF4, TLR2/4
	Cell cycle	1.86E-03–4.31E-02	6	BAX, CDKN2C, IL6, PRKCA/B, PPARα
	Cell-to-cell signaling and interaction	1.86E-03–4.37E-02	9	CSF1, NOS1, KCNH2, SNCA, TLR2/4
	Energy production	1.86E-03–4.31E-02	6	ADH4, ALDH1A1, HSD17B2, PPARα, SLC16A7, RDH16

tors of MAPK signaling were identified (e.g. IL7/10/27, IL3RA, IL4R, IL1RAAPI1/2, FOS, TGFBR1, TNFRSF13B/18, hypoxia-inducible factor, MAPK3, MAP2K3/4, JUNB/D, FOS, etc.; see Tables 2 and 3). Some of the significantly changed genes sub-

mitted to IPA as well as the genes mapped to cluster 1 or 2 (data not shown) were used for subsequent analyses. Overrepresented signaling pathways following plasma treatment were not only genes of MAPK, NRF2, and antioxidant response signaling but also genes of p53, transforming growth factor (TGF)-β, PPARα, retinoic acid receptor activation, and cell cycle G<sub>1</sub> checkpoint regulation. Further pathways dealing with the regulation of downstream targets were found in plasma-modulated groups, e.g. protein kinase C (PKC), phosphatidylinositol 3-kinase (PI3K), and the Janus kinase/signal transducers and activators of transcription (JAK/STAT) pathways. For longer treatment times, we found a regulation in neuronal NOS and MSP-RON signaling pathways, which play important roles in

inflammation and the late stages of wound healing (see details in Table 2).

With the assistance of IPA, the differentially expressed transcripts were organized and classified into networks. Although

## Plasma Triggers Hormesis-like Processes in Keratinocytes

many of the networks are commonly involved in gene expression, cellular function, growth, and proliferation, one of the top networks also includes those that contribute mainly to “cellular and connective tissue development and molecular transport” for the 3-h and 180-s groups as well as “small molecule biochemistry” for the 6-h group. In this context, networks discover an induction of targets of the JUN pathway within the transactivation of HMOX1 on mRNA (data not shown). We then asked what underlying molecular and cellular functions are associated with the mode of action in plasma-induced activation of cellular signal transduction. IPA annotation revealed that plasma was significantly involved in nucleic acid metabolism (3 and 6 h), small molecule biochemistry (3 and 6 h), cell signaling (3 and 6 h), cellular growth and proliferation (3 and 24 h), cellular development (3 and 24 h), cell-to-cell signaling and interaction (6 and 24 h), amino acid metabolism (6 h), and energy production (24 h) (see details in Table 3).

*Non-thermal Plasma Activates Phase II Enzymes through NRF2 Pathway to Scavenge ROS*—To confirm NRF2 signaling on single cell level, we analyzed subcellular localization of NRF2 after plasma exposure. HaCaT cells were incubated with the plasma-treated medium for the indicated period of time. Immunofluorescence staining with anti-NRF2 antibody has shown that protein translation is actively switched on after plasma treatment and that this is partly due to the activation of NRF2. This intracytosolic transcription factor is in its reduced form bound to KEAP1 (data not shown). Thus, untreated cells showed predominantly localization of NRF2 in the cytosol (Fig. 6, A–E). As expected, we confirmed the cytoplasmic-nuclear trafficking of endogenous NRF2 after plasma (Fig. 6, AI–EI) and H<sub>2</sub>O<sub>2</sub> treatment (100 μM; Fig. 6, AII–DII) by immunofluorescence microscopy. These findings were also verified and confirmed in primary NHEK cells by indirect immunofluorescence staining of NRF2. Upon 60 s of non-thermal plasma treatment of NHEK cells, NRF2 is released and translocates into the nucleus where it binds to specific DNA elements. In the untreated sample, there was no increase in NRF2 expression or nuclear accumulation visible (Fig. 6F).

To further study the role of NRF2-mediated antioxidant response and plasma-induced changes in redox balance, we performed qPCR and Western blot analysis of NRF2 and KEAP1. All time points were chosen for further analysis of plasma treatment time-dependent gene expression. In concordance with the results obtained from microarray and LC/MS, transcript and protein levels of NRF2 and KEAP1 were not significantly altered after longer incubation times (3–24 h). NRF2 and KEAP1 expression levels were mainly enhanced after very short incubation times (about 20 min; Fig. 7). However, applying immunofluorescence microscopy, no significant changes were seen in the expression and localization of KEAP1 in untreated cells (Fig. 7C, upper panel) and cells after plasma treatment (Fig. 7CI).

The results obtained by microarrays and LC/MS showed an activation of the downstream targets of NRF2 in plasma-treated keratinocytes. Corresponding to NRF2 activation, enhanced levels of HMOX1 and NQO1 mRNA were exclusively associated with the presence of plasma. Furthermore, a robust increase in protein expression of NQO1 was found in the pro-

teome approach (Fig. 4, left). To verify potential downstream activation of NRF2 target genes, a time course of the gene expression was assessed using qPCR. The expression of HMOX1 and NQO1 mRNA was induced in a treatment time-dependent manner. HMOX1 gene expression showed a maximal 12-fold up-regulation after 180 s of plasma treatment (Fig. 8A). NQO1 was up-regulated up to 2-fold after 60 s of plasma treatment (Fig. 8AI). Gene expression no longer increased with plasma treatment times longer than 60 s. Western blot analysis confirmed these findings: NQO1 protein was found to be increased after plasma treatment in the analyzed data set, whereas HMOX1 protein was at most 2-fold higher in comparison with control (Fig. 8, B and BI).

A treatment time-dependent increase in enzyme activity of NQO1 was detected. Treatments with 10 μM H<sub>2</sub>O<sub>2</sub> or 20-s plasma led to a measureable enzyme activity increase. NQO1 enzyme is synthesized *de novo*; this effect can be observed after 24 h only; after 6 h, no effect was seen (Fig. 9, A and A'). After 24 h, the inverse effect from expectations was measured for GPX enzyme activity. For intense treatments, enzyme activity was decreased. After 3 h, there was a slight increase in enzyme activity for moderate treatment intensities, whereas longer treatment time did not result in any measureable changes. After 6 h, no effect could be detected (Fig. 9, B–B'').

*Inhibitory Effect of siRNA on ARE Activity in Keratinocytes*—With non-thermal plasma as a regulatory agent causing a gene response, we found a potent modulator of NRF2 activity and its downstream signaling. To better understand how plasma impacts NRF2-ARE signaling, we used an siRNA transfection assay to knock down target genes of the NRF2/KEAP1 pathway in HaCaT cells. As shown by immunofluorescence, at the 72-h time point after transfection with siRNA directed against NRF2, NRF2 was decreased in treated samples compared with the non-transfected control group (Fig. 10B). Quantification by qPCR was done, and representative pictures of knockdown are shown: siRNA silencing directed against NRF2 led to a significant decrease in NRF2, KEAP1, HMOX1, and NQO1 expression in all samples (Fig. 10C). Interestingly, a number of other transcripts were down-regulated following knockdown, suggesting that NRF2 may control certain repressor activities. The mRNAs whose expression decreased most included PRDX1, which was reduced to 48%; SOD1 and SOD2, which were reduced to 34 and 69%, respectively; and GCLC and GCLM, which were reduced to 24 and 27%, respectively. Comparable silencing effects of KEAP1 knockdown were obtained for genes of the antioxidant defense system (e.g. PRDX1, SOD1/2, GCLC, and GCLM), whereas expression of catalase and growth factors HBEGF and VEGFA was enhanced (Fig. 10D).

Because BACH1 is a repressor of the oxidative stress response, we examined the function of BACH1 in HaCaT cells subjected to plasma exposure. It is not clear which ARE-driven genes are regulated by BACH1 after plasma exposure in HaCaT cells. Immunofluorescence of BACH1 following plasma treatment has shown a cytoplasmic as well as nuclear staining (data not shown). qPCR revealed a strong effect after knockdown of BACH1 on ARE-driven gene expression by studying HMOX1 as BACH1 is known to repress this oxygenase gene (34).

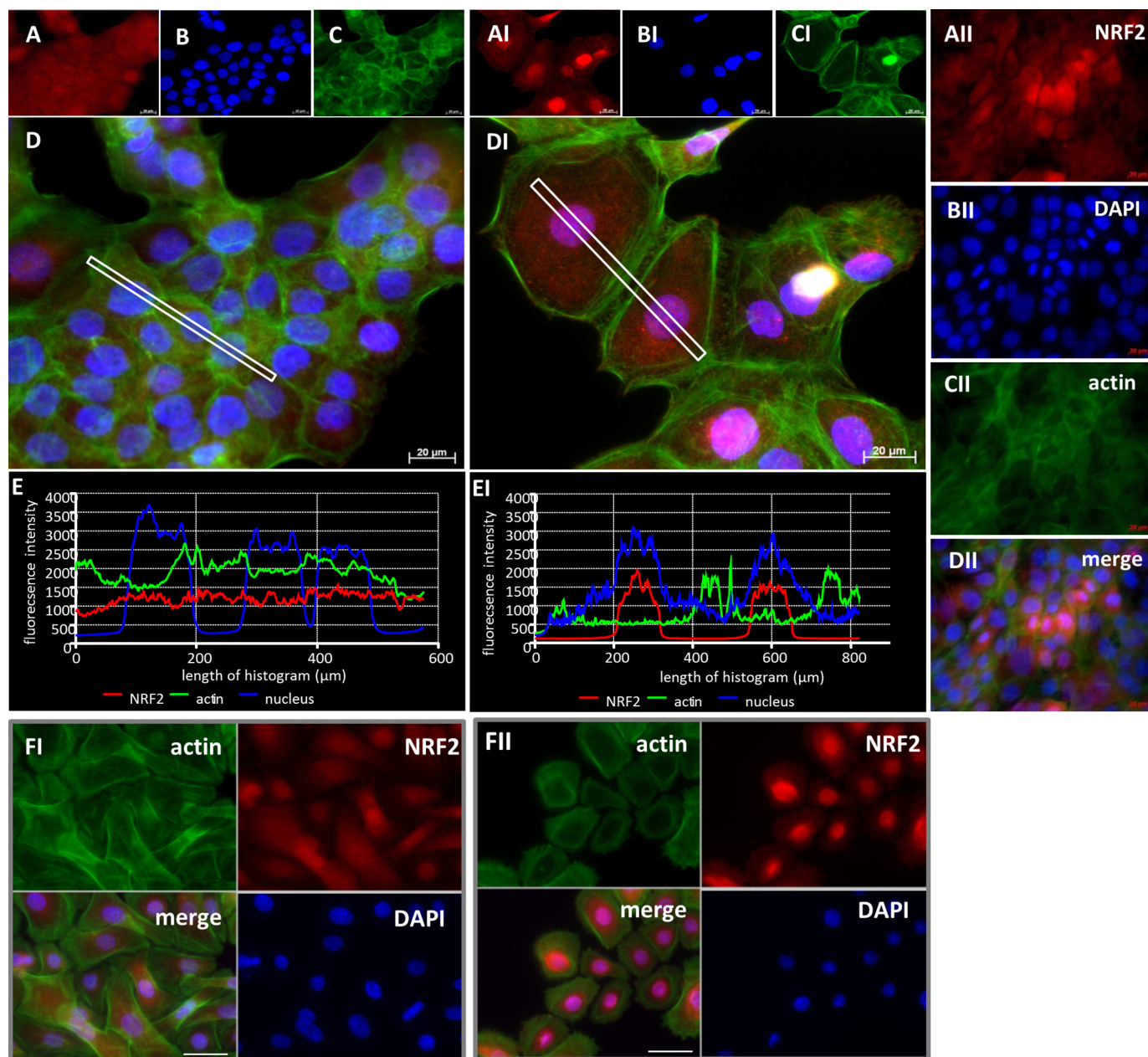


**FIGURE 6. The cytoplasmic-nuclear trafficking of NRF2 after non-thermal plasma treatment in HaCaT and NHEK cells.** Untreated cells are depicted in the left panels (A–E). Cells were incubated with plasma-treated medium for 60 s (15-min incubation; middle panels, AI–EI). Cells were treated with 50  $\mu\text{M}$   $\text{H}_2\text{O}_2$  (AII–DII). Subcellular localization of NRF2 was detected by indirect immunofluorescence staining with anti-NRF2 (red; A) and visualized with fluorescence microscopy. The nuclei were counterstained with DAPI (blue; B), and the actin cytoskeleton was stained with phalloidin-FITC antibody (green; C). The merged images are shown in D and DI. A histogram of the subcellular distribution of NRF2, actin, and nuclei (long rectangular box in D and DI, respectively) is shown in E and EI. F, the NRF2 staining was identical when performed in NHEK cells (green, actin cytoskeleton; red, NRF2; blue, DAPI). Scale bars, 20  $\mu\text{m}$ .

*HMOX1* was up-regulated 12-fold following *BACH1* silencing and is therefore negatively controlled by this protein to a much greater extent than had been observed for any of the genes controlled by KEAP1. Relative to *HMOX1*, only very modest increases of 2–2.5-fold in the mRNA were observed for *CAT* and *VEGFA* mRNA (Fig. 10E), and no increase was detected for *NQO1* mRNA (data not shown).

Next, we performed knockdown in the presence and absence of plasma treatment using siRNA directed against NRF2 genes. As demonstrated, non-thermal plasma induces nuclear translocation of NRF2 (Fig. 11A). NRF2 gene silencing (72 h before

plasma exposure) using siRNA abrogates the ability of plasma to increase mRNA for both enzymes after 20 min of cell incubation (Fig. 11B). In contrast, the exposure of cells to prolonged plasma treatment time (180 s) showed a clear increase of silenced NRF2 and accumulation in the cytoplasm as well in the nucleus of HaCaT cells (Fig. 11C).

## DISCUSSION

Given its potential to kill microorganism and to interact with cells or tissues, non-thermal atmospheric pressure plasma

## Plasma Triggers Hormesis-like Processes in Keratinocytes

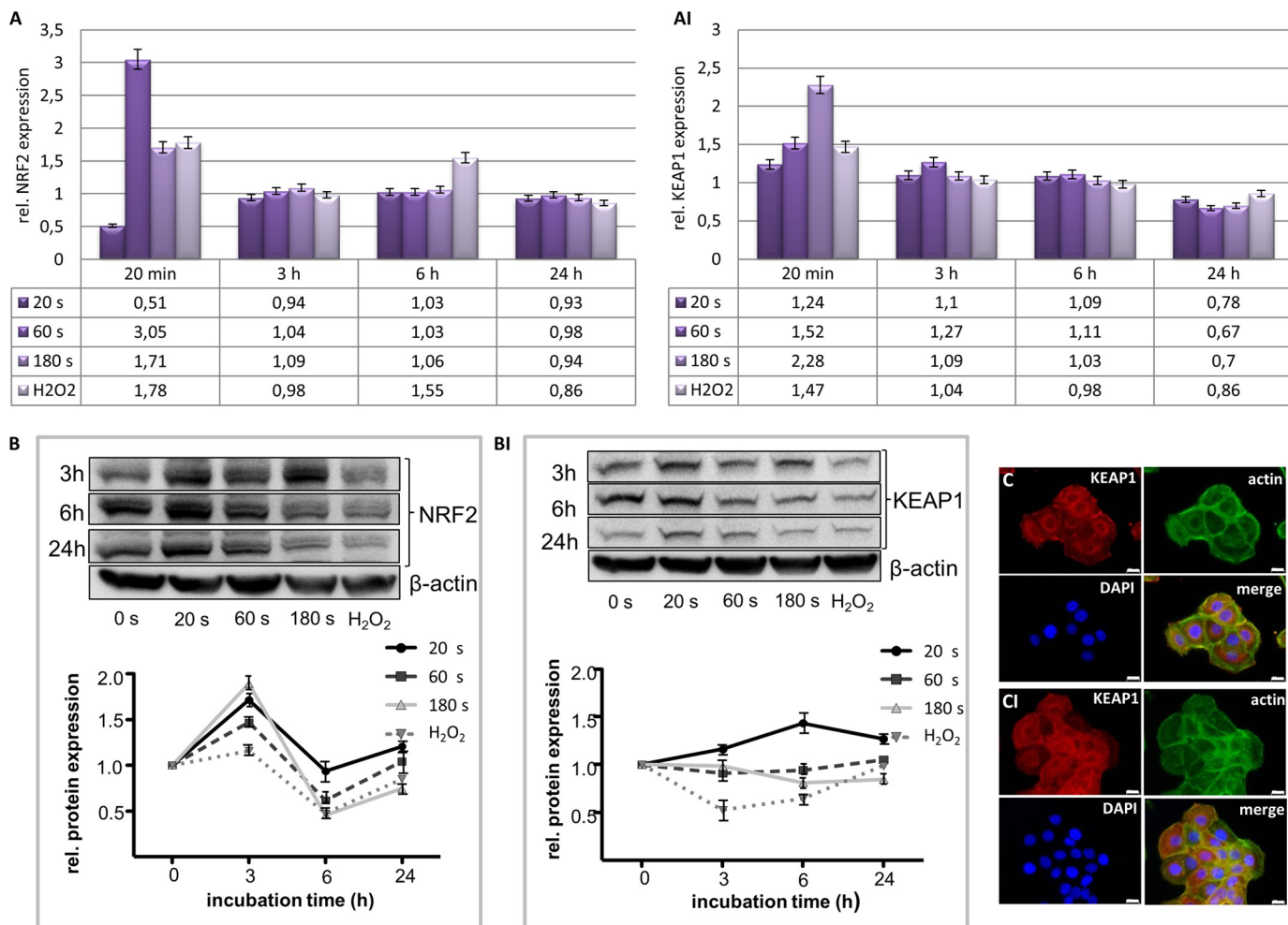


**FIGURE 7. Validation of the expression of target genes by qPCR.** HaCaT cells were plasma- or  $H_2O_2$ -treated for the indicated times. qPCR was performed for *NRF2* (A) and *KEAP1* (AI). B, representative Western blot analysis of *NRF2* (B) and *KEAP1* (BI) protein expression. Error bars represent S.D. of three independent measurements. C, immunofluorescence of cytoplasmic *KEAP1* expression before (C) and after plasma treatment (CI) in HaCaT cells. Scale bars, 50  $\mu$ m. rel., relative.

appears to be a promising biomedical tool for the treatment of various skin diseases including chronic wounds (24–26, 43). In this study, we investigated its effects on mRNA and protein levels to identify possible applications of non-thermal plasma in keratinocytes, e.g. in acceleration of wound healing and re-epithelialization. Thus, detailed knowledge about molecular signaling and the identification of responsible genes or proteins may represent valuable clinical targets for a wound therapy.

Although hydrogen peroxide is known for its cytotoxic effects, in recent years, it has been shown to play a crucial role in eukaryotic signal transduction (44).  $H_2O_2$  is an important second messenger for growth factors released during the wound healing process and has been shown to increase keratinocyte viability and migration in a wound model (45). Plasma-generated reactive intermediates add to the cellular production level of endogenous ROS (7). Regarding this, a notable fact is that reactive species are produced in the gas phase of the plasma jet itself; then they are solved in the liquid or secondary intermediates formed in the plasma-treated solution (46). Importantly,  $H_2O_2$  is a principal component of the “plasma mixture” produced by the kinpen (47). The highest plasma treatment (180 s) led to the production of about 100  $\mu$ M  $H_2O_2$  in the treated medium volume. The intracellular ROS level was up to 4 times

higher in comparison with control and leads to an increased sensitivity of treated cells to plasma. However, human cells have to be treated with caution because very high amounts of ROS/RNS generated by longer plasma treatment may inhibit cell growth or induce apoptotic pathways (48). Nevertheless, no differences in survival of plasma-treated HaCaT cells were detected under the treatment regimen chosen for this study. Moreover, apoptotic effects were nearly negligible at all treatment times. In a previous study, it was demonstrated that incubation of cells with plasma-treated medium resulted in an acute death rate under 10% in HaCaT cells (49), which was confirmed by the present data from viability assays. However, the magnitude of apoptosis is strongly dependent on the investigated cell type. Monocytes are less sensitive than  $CD4^+$  T helper cells, whereas Jurkat and THP-1 immune cells displayed a higher survival rate compared with their human blood counterparts (50).

The cellular effects of non-thermal plasma have been demonstrated *in vitro* in a variety of cell types (e.g. keratinocytes (39, 51), fibroblasts (52), and immune cells (1, 35, 50, 53)). However, knowledge about cellular signaling events in plasma-treated human cells is still rudimental. In this study, a global gene expression microarray analysis was performed to understand

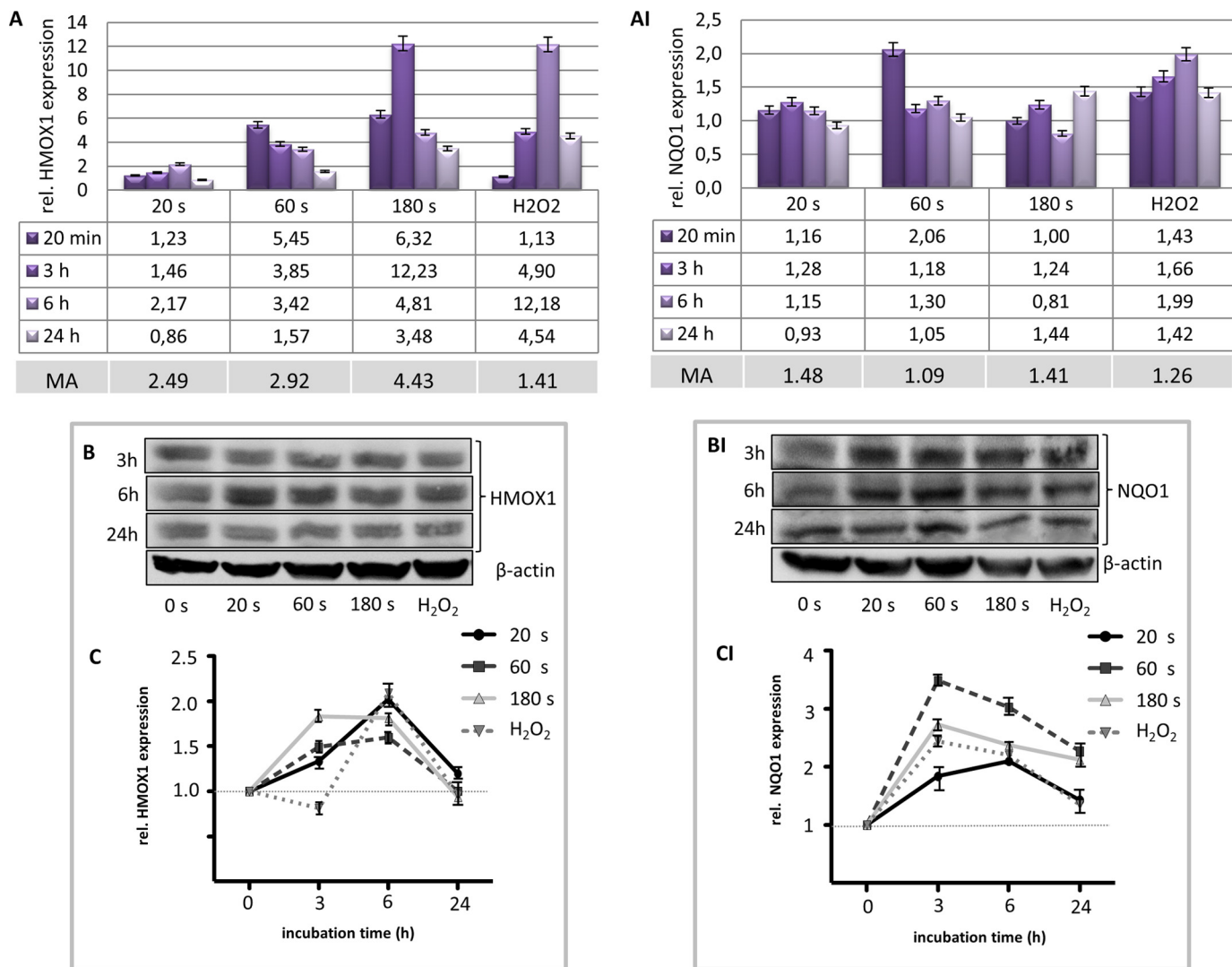


FIGURE 8. Plasma-induced regulation of HMOX1 and NQO1 antioxidant enzymes. A, qPCR analysis of the plasma effect on HMOX1 and NQO1 mRNA expression in HaCaT cells. Results from qPCR confirmed mRNA gene expression of HMOX1 and NQO1 measured in microarrays (MA; bottom lane in tables). B, representative Western blot analysis of the plasma effect on HMOX1 (B) and NQO1 (BI) protein expression for all time points indicated. Error bars represent S.D. of three independent measurements.

the whole transcriptional response of the human keratinocyte cell line HaCaT to non-thermal plasma and to analyze the total cellular proteome under the same conditions. An indirect treatment with an argon-driven plasma jet was done to identify correlation of intracellular signaling with duration of plasma treatment and subsequent incubation time as well as correlation between mRNA and protein expression. Because ROS/RNS are generated by non-thermal plasma, the question was how plasma triggers the transcription and translation of oxidative stress-responsive proteins to contribute as an agent that promotes wound healing.

Primarily, we assessed the levels of 24,000 transcripts in plasma-treated HaCaT cells and obtained marked alterations in the expression of hundreds of genes in all experimental groups (data set GSE58395). Upon plasma treatment, HaCaT cells regulated many more genes in the 6-h group compared with the 3- or 24-h group or with immune cells (50), indicating that the highest changes in gene expression activity occurred after medium term incubation time. A possible explanation for the

higher number of regulated genes in HaCaT cells in contrast to plasma-treated immune cells could be that the latter have a totally different behavior regarding oxidative stress events: e.g. monocytes produce reactive species themselves (54). Moreover, the distribution of genes depicted in Venn diagrams clearly shows that the incubation time of plasma is much more important than the treatment time between 20 and 180 s. This finding supports the assumption that plasma-generated stable species in liquids induce the cellular response (55). Additionally, plasma-activated reactions were obtained up to several hours after plasma treatment in post-treatment kinetic measurements (56).

Summarizing identified changes, the altered transcripts were classified into several categories according to their functional roles. Among others (e.g. metabolism, transport, and redox homeostasis), the regulation of transcription, signal transduction, and antioxidant activities belong to classes with the most alterations. The vast bulk of induced or repressed genes after plasma treatment include transcription factors, receptors, sig-

## Plasma Triggers Hormesis-like Processes in Keratinocytes

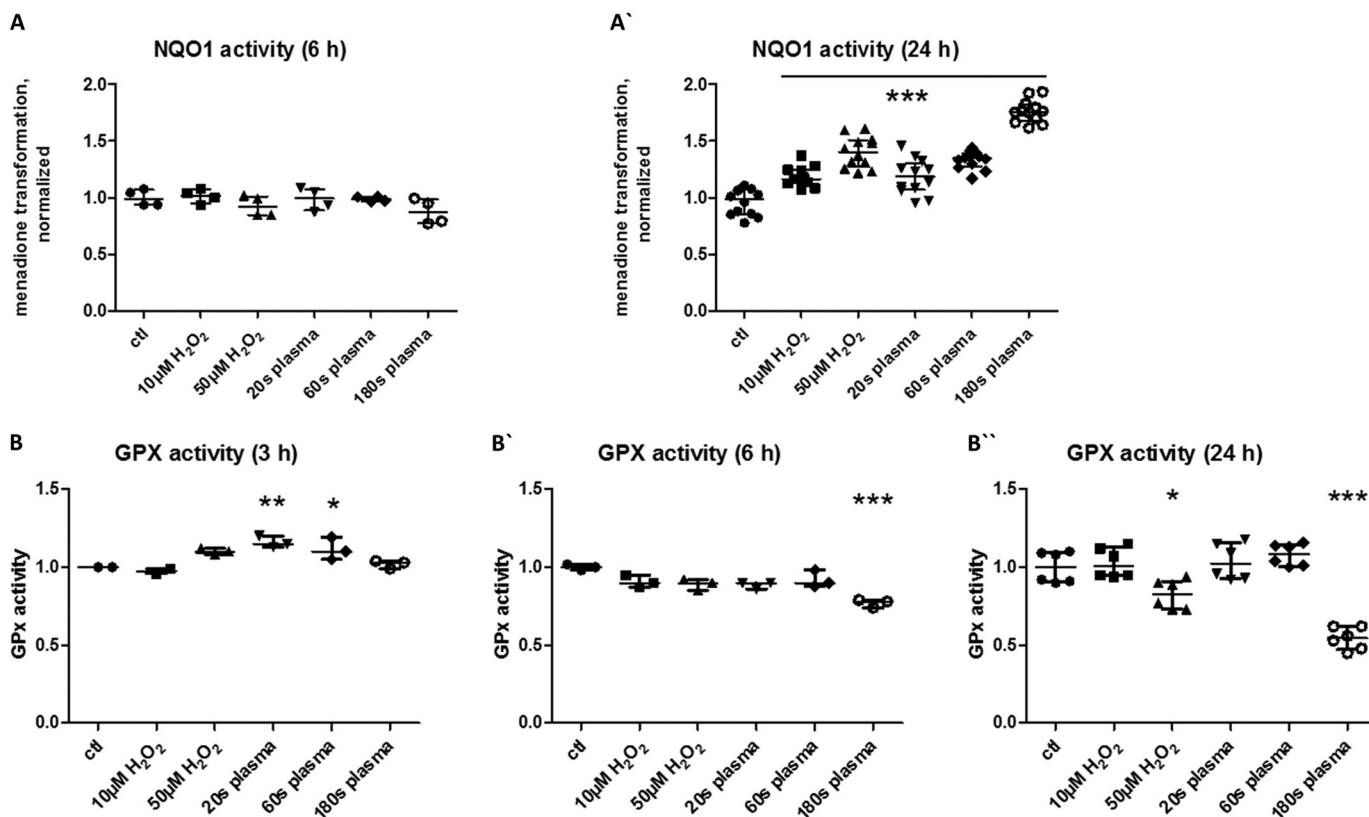


**FIGURE 9. Enzyme activity of NQO1 and GPX.** *A*, NQO1 activity after 6 (*A*) and 24 h (*A'*) after plasma treatment. A treatment time-dependent increase in enzyme activity was detected. *B*, glutathione peroxidase activity after 3 (*B*), 6 (*B'*), and 24 h (*B''*). After 3 h, a treatment time-dependent increase was detected, whereas after 6 h, no effect on GPX activity was measured. After 24 h, a decrease for long treatment times was observed. Error bars represent S.D. *ctl*, control. \*,  $p \leq 0.05$ ; \*\*,  $p \leq 0.01$ ; \*\*\*,  $p \leq 0.001$  (Tukey HSD).

naling molecules, and genes involved in antioxidant activity such as oxidoreductases (7). Additionally, 350 (down-regulated) and 400 (up-regulated) proteins were identified by LC and MS. Analysis of the proteome data set showed for the plasma-treated cells a comparable normal cell physiology as was indicated by eIF2 signaling, eIF4/p70S6K signaling, or transfer RNA charging (protein translation, etc.). The protein ubiquitination pathway was found to be emphasized. This is in agreement with increased demand of protein degradation provoked by oxidative (or other plasma chemistry-derived) modification of proteins. From this perspective, the active protein *de novo* synthesis machine might result from increased protein degradation and demonstrates the necessity to replace proteins. Overall, by LC/MS, 10% of proteins were found to be regulated by the plasma treatment: among the most regulated proteins identified were antioxidant-acting factors and enzymes (42). In accord with this finding, the regulatory effects of plasma on genes and proteins of the antioxidant defense system or on molecules involved in redox homeostasis were the focus of our investigations.

An increased abundance of intracellular reactive species needs to be controlled by the cell. An important switch to control ROS and/or RNS levels is the intracytosolic transcription factor NRF2, which in its reduced form is bound to KEAP1 (57). By IPA prediction, NRF2 signaling was ranked among the most active regulatory network and canonical pathway (Fig. 11D). For the data sets of gene activation, 16 NRF2 targets were

found in the 20-s group, 16 molecules were found in the 60-s group, 26 molecules were found in the 180-s group, and most were predominantly in the 3-h incubation group. For the protein expression data set, the most NRF2-regulated proteins were found after 24 h.

Transcript and protein levels of NRF2 were mainly enhanced after short incubation times (20 min or 3 h, respectively; Fig. 7, *A* and *B*). The fluctuating expression may result from a negative feedback loop fed by the increased expression of antioxidant proteins and the accordingly increased ubiquitination of the protein. However, similar to oscillating p53 expression (58), fluctuating NRF2 protein expression may also reflect a modulation of the antioxidative response intensity or may be necessary for the specific function of individual NRF2 targets. Data from Pekovic-Vaughan *et al.* (59) revealed a rhythmic nuclear abundance of endogenous NRF2 protein in tissues and cells that accompanies the rhythmic levels of the total pool of NRF2 protein. We suggest that the function of NRF2 is to act as a key molecule that promotes and maintains transcriptional noise to interfere with stress signals evoked by plasma treatment. These results suggest that alterations in the status of ROS intermediates dependent on chemical reactions in liquids (55) cause fluctuations in expression levels of such signaling molecules.

Consistent with the expression pattern in the literature (29, 60, 61), NRF2 immediately translocates to the nucleus in response to plasma and binds to ARE sequences in the promoters of its target genes. Afterward, a significant mRNA expres-

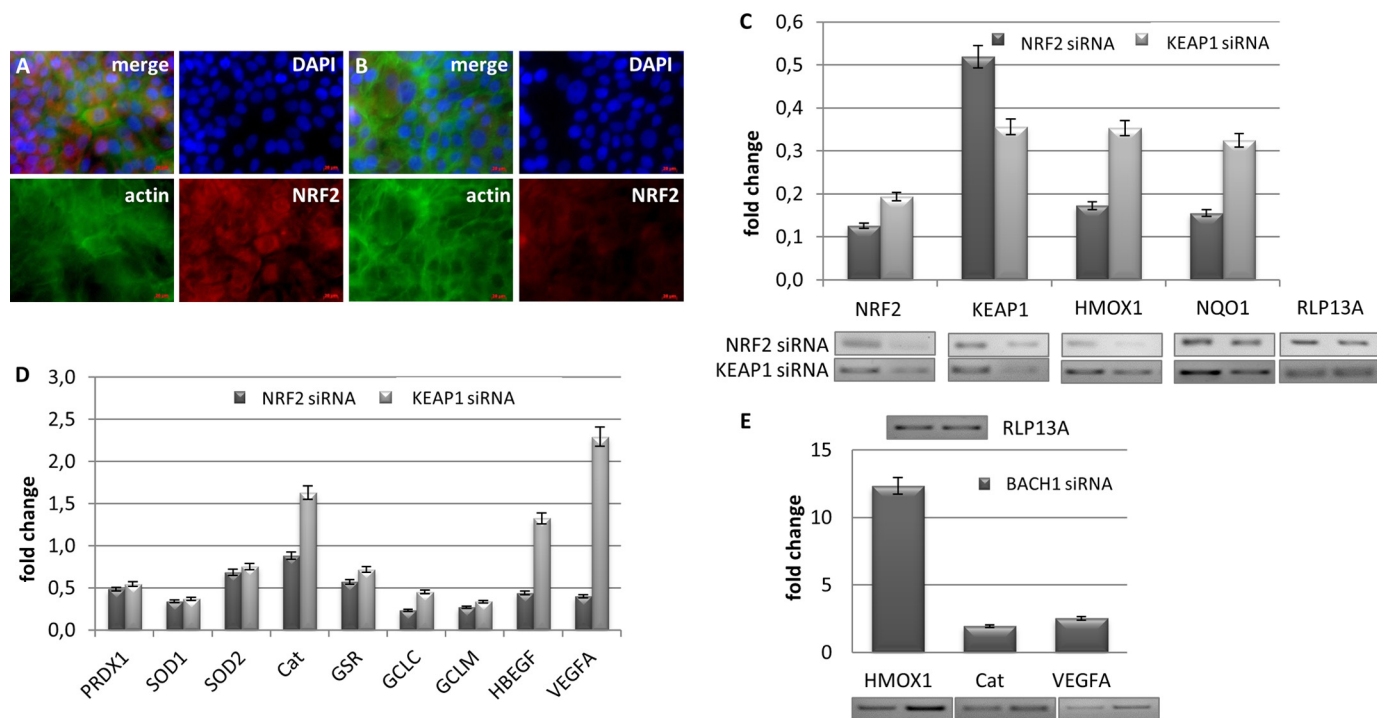


FIGURE 10. **Representative pictures of immunofluorescence microscopy of the effect of NRF2 siRNA on NRF2 expression.** A and B, HaCaT cells were transfected with a control scrambled siRNA (A) or NRF2 siRNA (B) and incubated for 72 h. Red scale bars, 50  $\mu$ m. C, quantification of qPCR of NRF2 and KEAP1 siRNA knockdown. Representative semiquantitative PCR images for NRF2 and KEAP1 siRNA knockdown for NRF2, KEAP1, HMOX1, and NQO1 are shown. D, qPCR of different enzymes of antioxidant defense enzymes after knockdown of NRF2 and KEAP1. E, BACH1 siRNA knockdown led to a significant up-regulation of HMOX1, CAT, and VEGFA. Error bars represent S.D. of three independent measurements.

sion of antioxidant and phase II detoxification enzymes and proteins such as GPX, CAT, SOD, HMOX1, NQO1, mitogen-activated protein kinases, and molecules of the JUN pathway was triggered. Therefore, NRF2 acts as an important switch for sensing oxidative stress events triggered by the plasma treatment. Furthermore, the result showed that protein translation is actively switched on and that this is partly due to the activation of NRF2. For example, NQO1, a member of the NADPH dehydrogenase family encoding a cytoplasmic two-electron reductase gene, and carbonyl reductase 1 were shown to be significantly increased after plasma treatment. In perfect correlation with global measurements, we also found a treatment time-dependent increase in enzyme activity of NQO1. However, there was a slight divergence between transcriptomic data (global and qPCR) and proteomic data (Western blot and LC/MS) observed that might be explained as follows. NQO1 as a major cellular antioxidant is permanently transcribed in metabolically active cells. As protein accumulates, it may act as a repressor of transcription and signaling. Accordingly, an increase in transcription might not be necessary for shorter plasma treatment times. In addition, a fast ubiquitination of NQO1 is described for a one-amino acid polymorphism (NQO1\*2) (62). In this case, the half-life time of the enzyme drops from 18 (wild type) to 1.2 h. One may speculate that a similar, but not yet identified, mechanism may be in charge of controlling the NQO1 levels during normal conditions. In this case, excess NQO1 would be degraded by a proteasomal mechanism. With rising oxidative stress, ubiquitination decreases, and protein stability increases. This would lead to the situation observed: although mRNA levels remain at the control rate,

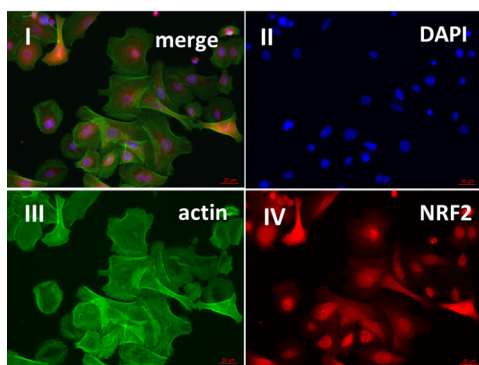
protein degradation stops under stimulus (plasma), and apparent protein expression increases. If stimulus keeps rising, transcription soars as do protein level and activity with both global gene and proteome data now in accordance. The strongly up-regulated carbonyl reductase 1 is involved in nitrosoglutathione recycling, hinting at a possible role for RNS in this scenario (46).

Nevertheless, the expression of enzymes involved in glutathione synthesis such as GCLC/GCLM was not found to be up-regulated after 3–24 h. Other proteins like heat shock proteins (HSP90s and HSP40s) and cytosolic and membrane-bound forms of glutathione S-transferase (GSTO1) show an increased abundance regardless of sampling time (up to 24 h). HSPs are observed after cellular stress and serve mainly to prevent misfolding or aggregation of cellular proteins (42). GSTs function in the detoxification of electrophilic compounds including products of oxidative stress by conjugation with glutathione (63).

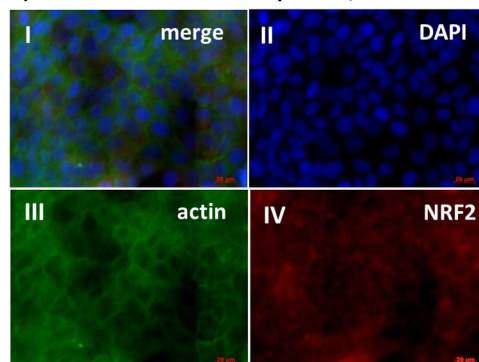
GPX shows a more complex behavior than NQO1. The protein activity seems to be in poor correlation with global gene or protein data, which both indicate an increase in expression. One possible explanation could be that GPX needs to be processed before being active: the active center selenocysteine is included in a posttranslational mechanism. If selenium is limited in the assay medium, the production of functional protein might be reduced. Additionally, the potential oxidation of selenium to selenium oxide could lead to GPX inactivation as selenium is equally likely to be oxidized as sulfur (64). Therefore, we detected a slight reduction of GPX enzyme activity especially in the case of longer treatment.

## Plasma Triggers Hormesis-like Processes in Keratinocytes

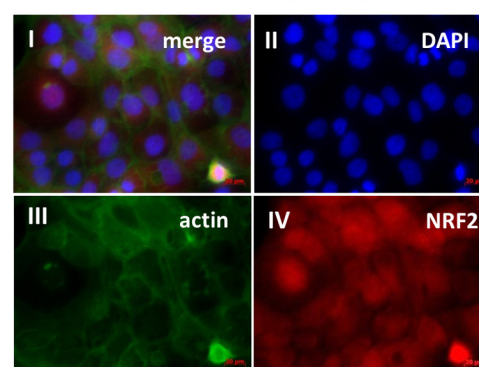
### A) 60 s plasma treatment, 20 min incubation



### B) NRF2 knockdown + 60 s plasma, 20 min incubation



### C) NRF2 knockdown + 180 s plasma, 1 h incubation



### D

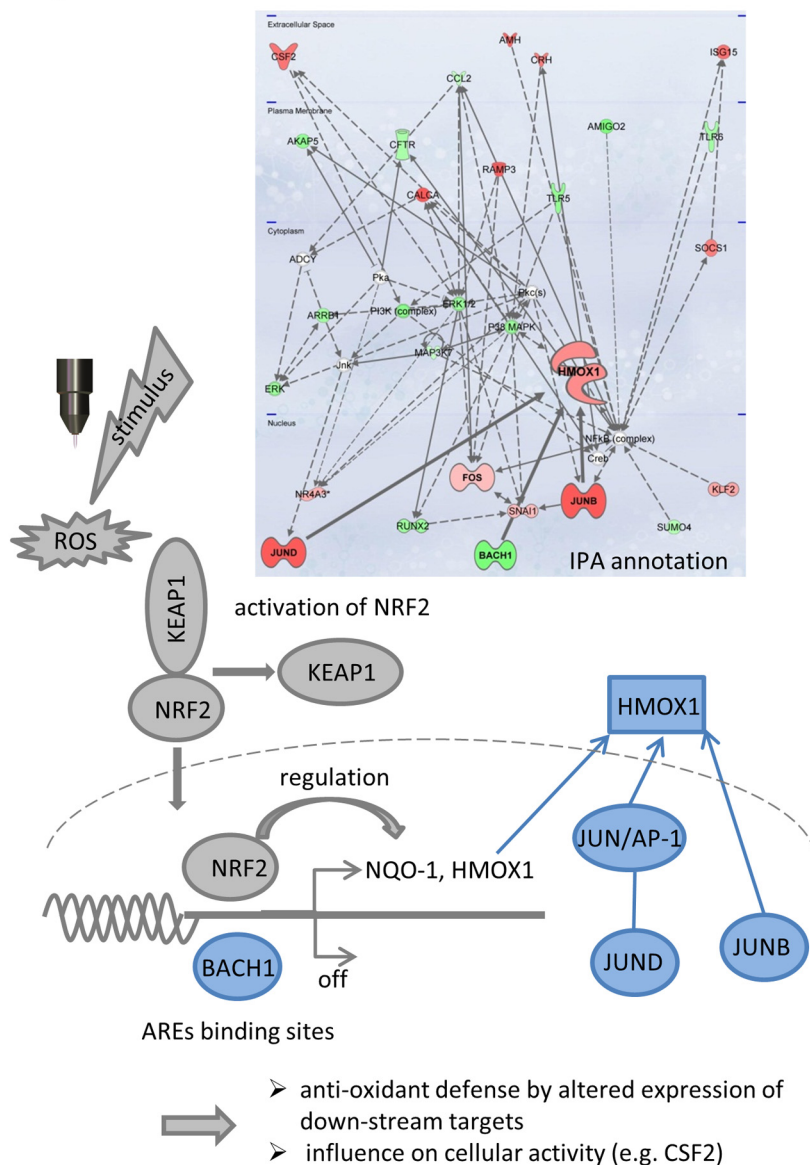


FIGURE 11. **Plasma treatment abolish siRNA-induced knockdown of NRF2.** *A, I–IV*, immunofluorescence microscopy showing nuclear trafficking of NRF2 after plasma treatment. *B, I–IV*, HaCaT cells were transfected with a control scrambled siRNA or NRF2 siRNA and incubated for 72 h. After 60-s plasma treatment (20-min incubation), plasma effects on NRF2 localization were obtained. *C, I–IV*, increased plasma treatment time up to 180 s and prolonged incubation time (1 h) abolish siRNA-induced knockdown of NRF2 and enhanced expression of NRF2 in the cytosol and the nuclear translocation. *D*, functional annotation, pathway, network analysis, and graphical summary of NRF2 activation in keratinocytes after plasma treatment. The top gene interaction networks associated with plasma-treated HaCaT cells were predicted by IPA and are presented for all groups. About 30 genes are involved in the network. A *solid line* represents a direct interaction and a *dashed line* represents an indirect interaction between target genes (*red*, up-regulation; *green*, down-regulation). Plasma activates NRF2 signaling and induces an antioxidant response. Among others, HMOX1, FOS, JUN, JUNB/D, and BACH1 were regulated by plasma. Regulation of several components is simplified in the drawing.

Plasma treatment quickly changed the mRNA status of *KEAP1* but did not change the protein expression level after longer treatment times. Hydrogen peroxide marginally decreased the levels of KEAP1 protein after 3 h, indicating its ubiquitin-dependent proteasomal degradation. We concluded that only concentration-dependent differences were detected. Nevertheless, slight differences between reactions with plasma and those with  $H_2O_2$  in regard to KEAP1 expression are consistent with the fact that many other compounds (secondary radicals) in plasma interact with cells and provoke differences in their gene and protein expression (46, 47, 55).

The induction of cytoprotective enzymes in response to stress was regulated primarily at the transcriptional level. The argon plasma treatment produced a significant increase in *HMOX1* mRNA levels up to 12-fold. The outcome of this is that HMOX1 activity is not only induced by its substrate heme but also by non-heme substances such as plasma. In oxidative environments like skin injury or wounds,  $H_2O_2$  releases the potent oxidant agent heme, which is degraded by HMOX1 to iron ion, carbon monoxide (a putative neurotransmitter), biliverdin, and bilirubin (66). The HMOX1 promoter is known to contain multiple ARE binding motifs, suggesting transcriptional regulation

not only over AP-1 but also over NRF2 (67). The heme-HMOX system including transporters and degrading and binding proteins of heme as well as antioxidant enzymes protects the skin from heme, which contributes to several diseases (68). Additionally, it was shown that HMOX1 influences wound healing, especially in vascularization (69), and plays an important role in the regulation of vascular endothelial growth factor expression (70, 71). Therefore, evidence is accumulating that the heme-HMOX system forms a novel and important target in plasma applications. However, HMOX1 could not be detected by LC/MS, whereas HMOX2 was found. Analysis of the identified peptides indicated that, although both enzymes share a high homology, no disambiguation occurred. Either HMOX1 is translated later than 24 h after treatment or in a small amount only, or it might result in no distinct peptides, hampering LC/MS detection.

To show functional relevance of the plasma-induced NRF2 pathway in HaCaT cells, the effect of NRF2 and KEAP1 silencing on expression of antioxidant enzymes was investigated. The finding that NRF2 inhibition by siRNA silencing results in down-regulation of phase II gene induction program in HaCaT cells (Fig. 10) supports the importance of NRF2 in cellular defense. A lack of NRF2 is associated with heightened sensitivity to oxidative stress (72, 73). In contrast, the activation of NRF2 by plasma treatment after silencing (Fig. 11C) leads to an activation of many ARE-dependent target genes (e.g. *HMOX1*, *NQO1*, *SOD*, and *GSR*), suggesting a possible protection mechanism of non-thermal plasma against cytotoxic alterations in redox levels. Such mechanisms could support processes like wound healing in which signal molecules stimulate ongoing processes. Interestingly, KEAP1 knockdown did not activate the ARE gene battery. After silencing of KEAP1, we found a strong down-regulation of *NRF2*, *HMOX1*, and *NQO1*, showing that inhibition of KEAP1 is critical for regulation of intracellular redox conditions in keratinocytes. In contradiction to the literature, the cytosolic interaction between NRF2 and KEAP1 is such that if one of the interaction partners is knocked down (either NRF2 or KEAP1) the other is also down-regulated. One result of the knockdowns is that the ubiquitination of proteins can occur faster. Experiments by Itoh *et al.* (74) suggest a delicate balance of NRF2 protein stability due to its high turnover rate. The presence of KEAP1 was important to reduce proteasomal degradation. In contrast, we observed an increase in *VEGFA* expression after KEAP1 knockdown, indicating roles of NRF2 other than the antioxidative protection of cells (Fig. 10D). Interestingly, *VEGF* expression was indeed shown to be increased by plasma treatment in the cellular environment (49). This growth factor has multiple effector cells among which are keratinocytes and endothelial cells. In chronic wounds, increased oxygenation of the tissue is desirable. Our data indicate that this might be achieved by plasma treatment. Taken together, the interference of non-thermal plasma with the NRF2/KEAP1 axis prepares eukaryotic cells against exogenic noxae and increases their resilience against oxidative species. Via paracrine mechanisms, distant cells also benefit from cell-cell communication triggered by the treatment.

In contrast, BACH1 heterodimers function as repressors of gene expression by binding on AREs. Usually, BACH1 is inac-

tivated in the presence of oxidative stress, which allows transcriptional activation of genes by NRF2 and transcriptional repression in the absence of oxidative stress (75, 76). We found a plasma-induced repression of the function of BACH1, which evokes a preferential binding of NRF2 on AREs and an activation of target genes such as *HMOX1* (data not shown). Using knockdown directed against BACH1, we investigated the role of BACH1 as a potential target for oxidative gene expression regulation after plasma treatment. Data indicated that BACH1 silencing by small interfering RNA is associated with induction of genes like *HMOX1*, *VEGFA*, and catalase, indicating that BACH1 is a critical repressor of these genes in HaCaT cells. As expected, we demonstrated a strong, up to 12-fold increase in *HMOX1* expression, showing that BACH1, together with its competitor NRF2, regulates cellular responses to oxidative stress after plasma treatment through specific induction of HMOX1.

Taken together, we propose that a plasma stimulus resulting in ROS generation leads to an activation of the transcription factor NRF2 and to an antioxidant defense response by altered expression of downstream targets like HMOX1, NQO1, and BACH1 (Fig. 11D). Additionally, some proteins show distinctive incubation time dependence, e.g. different MAPKs. MAPK signaling was one of the most overrepresented pathways after plasma treatment on the gene as well as protein level. Moreover, several cell types showed a plasma-mediated activation of different mitogen-activated protein kinases, indicating that they are important intracellular plasma responses (50). MAPKs play an important role in wound healing (77), and they mainly regulate the phosphorylation of transcription factors (78). The p38 MAPK pathway is activated by a diverse array of stress stimuli that include inflammatory cytokines, death ligands (e.g. TNF), TGF- $\beta$ -related polypeptides, and environmental factors like oxidative stress (79). The response to stress by activation of those factors culminates in enhanced transcriptional activity and protein synthesis as we found by microarray and gel-free LC/MS proteomics (eIF2 signaling, eIF4/p70S6K signaling, or transfer RNA charging). Because an induction of JUNB/D and FOS could be identified in this study, the activation of AP-1 in the JUN pathway will be one possible activation mechanism following plasma treatment. A discrete increase of H<sub>2</sub>O<sub>2</sub> triggers most of the proliferation signaling pathways by activation of transcription factors like NF- $\kappa$ B, p53, RAF, hypoxia-inducible factor- $\alpha$ , glucocorticoid receptor, and AP-1 (80). The latter, AP-1, which belongs to the JUN family, is an inducible transcription factor and regulates gene expression in response to a variety of stimuli like ROS (81). AP-1 family members are involved in various molecular mechanisms inducing proliferation, differentiation, and cell fate determination (82). JUND was found to be essential for cytokine secretion, which is important for a proper wound healing (83). Furthermore, plasma accelerates the expression of the keratinocyte-derived granulocyte-macrophage colony-stimulating factor (CSF2). Both an up-regulated gene expression of *CSF2* and an increased secretion of its synthesized gene product, GM-CSF, as measured by ELISA (data not shown) were observed. An overexpression of *CSF2* suggests beneficial effects in wound healing (e.g. re-epithelialization) via the induction of secondary cytokines and has been shown to

improve wound healing by recruitment of leukocytes, enhance keratinocyte proliferation, and increase angiogenesis by VEGF up-regulation (49, 84).

Further understanding of the protection offered by NRF2 expression may provide clues to new modalities for *in vivo* skin protection and prevention of skin disorders. Stress tolerance and promotion of cell survival are increased by NRF2 activation (85). A decline in NRF2 function also sensitizes cells to oxidative stress during aging; increased NRF2 levels have been noted in the cells of long lived mice, and high NRF2 levels protect these cells against oxidant-induced damage. Several studies have suggested that the beneficial effects of chemopreventive drugs on the suppression of carcinogenesis are mediated through activation of NRF2 (86). In contrast, some studies suggest an oncogenic characteristic of NRF2 causing constitutive activation and resistance to chemotherapy (87). Just a transient (and not a permanent) activation of NRF2 by non-thermal plasma should not be associated with cancer formation. This assumption is in accordance with results of a colony transformation assay showing that plasma exposure of HaCaT cells has no cancerogenic properties (data not shown). Moreover, several plasma treatment times were used to analyze the mutagenicity induced in V79 Chinese hamster cells. Results of a hypoxanthine-guanine phosphoribosyltransferase mutation assay further show that plasma treatment did not induce mutagenicity at the *Hprt* locus (88).

By applying non-thermal plasma, it is feasible to manipulate cellular reactions simultaneously at diverse levels. Our data show that both gene and protein expression is highly affected by non-thermal plasma and highlight the pivotal role played by NRF2 in regulating cellular defenses against oxidative stress. Plasma-induced regulation of NRF2/KEAP1/BACH1 is a mechanism to induce multiple ARE genes and proteins in keratinocytes. These findings suggest that non-thermal plasma provides an interesting therapeutic tool to control redox-based processes, e.g. wound healing. Results are useful for the identification of molecular targets for novel therapeutic strategies in wound management. Plasma-based delivery of reactive oxygen and nitrogen species stimulates or inhibits cellular processes and triggers hormesis-like processes in keratinocytes.

*Acknowledgments*—We thank L. Kantz for distinguished technical support. For critical reading of the manuscript, we thank J. C. Schmidt. This work was realized within the framework of the multidisciplinary research center ZIK plasmatis, which is funded by German Federal Ministry of Education and Research Grant 03Z2DN11.

### REFERENCES

1. von Woedtke, T., Reuter, S., Masur, K., and Weltmann, K.-D. (2013) Plasmas for medicine. *Phys. Rep.* **530**, 291–320
2. Daeschlein, G., Scholz, S., Ahmed, R., von Woedtke, T., Haase, H., Niggemeier, M., Kindel, E., Brandenburg, R., Weltmann, K. D., and Juenger, M. (2012) Skin decontamination by low-temperature atmospheric pressure plasma jet and dielectric barrier discharge plasma. *J. Hosp. Infect.* **81**, 177–183
3. Brandenburg, R., Lange, H., von Woedtke, T., Stieber, M., Kindel, E., Ehlbeck, J., and Weltmann, K. D. (2009) Antimicrobial effects of UV and VUV radiation of nonthermal plasma jets. *IEEE Trans. Plasma Sci.* **37**, 877–883
4. Daeschlein, G., von Woedtke, T., Kindel, E., Brandenburg, R., Weltmann, K. D., and Junger, M. (2010) Antibacterial activity of an atmospheric pressure plasma jet against relevant wound pathogens *in vitro* on a simulated wound environment. *Plasma Process. Polym.* **7**, 224–230
5. von Woedtke, T., Kramer, A., and Weltmann, K. D. (2008) Plasma sterilization: what are the conditions to meet this claim? *Plasma Proc. Polym.* **5**, 534–539
6. Schmidt, A., Wende, K., Weltmann, K.-D., and Masur, K. (2013) Identification of the molecular basis of non-thermal plasma-induced changes in human keratinocytes. *Plasma Med.* **3**, 15–25
7. Schmidt, A., Wende, K., Bekeschus, S., Bundscherer, L., Barton, A., Ottmüller, K., Weltmann, K. D., and Masur, K. (2013) Non-thermal plasma treatment is associated with changes in transcriptome of human epithelial skin cells. *Free Radic. Res.* **47**, 577–592
8. Werner, S., Krieg, T., and Smola, H. (2007) Keratinocyte-fibroblast interactions in wound healing. *J. Invest. Dermatol.* **127**, 998–1008
9. Darr, D., and Fridovich, I. (1994) Free radicals in cutaneous biology. *J. Invest. Dermatol.* **102**, 671–675
10. Hanselmann, C., Mauch, C., and Werner, S. (2001) Haem oxygenase-1: a novel player in cutaneous wound repair and psoriasis? *Biochem. J.* **353**, 459–466
11. Vile, G. F., Basu-Modak, S., Waltner, C., and Tyrrell, R. M. (1994) Heme oxygenase 1 mediates an adaptive response to oxidative stress in human skin fibroblasts. *Proc. Natl. Acad. Sci. U.S.A.* **91**, 2607–2610
12. Kondo, N., Nakamura, H., Masutani, H., and Yodoi, J. (2006) Redox regulation of human thioredoxin network. *Antioxid. Redox Signal.* **8**, 1881–1890
13. Ristow, M., Zarse, K., Oberbach, A., Klötting, N., Birringer, M., Kiehnopf, M., Stumvoll, M., Kahn, C. R., and Blüher, M. (2009) Antioxidants prevent health-promoting effects of physical exercise in humans. *Proc. Natl. Acad. Sci. U.S.A.* **106**, 8665–8670
14. Sen, C. K. (1998) Redox signaling and the emerging therapeutic potential of thiol antioxidants. *Biochem. Pharmacol.* **55**, 1747–1758
15. Sen, C. K. (2003) The general case for redox control of wound repair. *Wound Repair Regen.* **11**, 431–438
16. Sen, C. K. (2009) Wound healing essentials: let there be oxygen. *Wound Repair Regen.* **17**, 1–18
17. Soneja, A., Drews, M., and Malinski, T. (2005) Role of nitric oxide, nitroxidative and oxidative stress in wound healing. *Pharmacol. Rep.* **57**, (suppl.) 108–119
18. Fridman, G., Shereshevsky, A., Jost, M. M., Brooks, A. D., and Fridman, A. (2007) Floating electrode dielectric barrier discharge plasma in air promoting apoptotic behavior in melanoma skin cancer cell lines. *Plasma Chem. Plasma Process.* **27**, 163–176
19. Graves, D. B. (2012) The emerging role of reactive oxygen and nitrogen species in redox biology and some implications for plasma applications to medicine and biology. *J. Phys. D Appl. Phys.* **45**, 1–42
20. Weltmann, K.-D., Kindel, E., Brandenburg, R., Meyer, C., Bussiahn, R., Wilke, C., and von Woedtke, T. (2009) Atmospheric pressure plasma jet for medical therapy: plasma parameters and risk estimation. *Contrib. Plasma Phys.* **49**, 631–640
21. Heinlin, J., Isbary, G., Stolz, W., Morfill, G., Landthaler, M., Shimizu, T., Steffes, B., Nosenko, T., Zimmermann, J., and Karrer, S. (2011) Plasma applications in medicine with a special focus on dermatology. *J. Eur. Acad. Dermatol. Venereol.* **25**, 1–11
22. Isbary, G., Morfill, G., Schmidt, H. U., Georgi, M., Ramrath, K., Heinlin, J., Karrer, S., Landthaler, M., Shimizu, T., Steffes, B., Bunk, W., Monetti, R., Zimmermann, J. L., Pompl, R., and Stolz, W. (2010) A first prospective randomized controlled trial to decrease bacterial load using cold atmospheric argon plasma on chronic wounds in patients. *Br. J. Dermatol.* **163**, 78–82
23. Isbary, G., Morfill, G., Zimmermann, J., Shimizu, T., and Stolz, W. (2011) Cold atmospheric plasma: a successful treatment of lesions in Hailey-Hailey disease. *Arch. Dermatol.* **147**, 388–390
24. Kramer, A., Lademann, J., Bender, C., Sckell, A., Hartmann, B., Münch, S., Hinz, P., Ekkernkamp, A., Matthes, R., Koban, I., Partecke, I., Heidecke, C. D., Masur, K., Reuter, S., Weltmann, K.-D., Koch, S., and Assadian, O. (2013) Suitability of tissue tolerable plasmas (TTP) for the management of chronic wounds. *Clin. Plasma Med.* **1**, 11–18

25. von Woedtke, T., Metelmann, H.-R., and Weltmann, K.-D. (2014) Clinical plasma medicine: state and perspectives of *in vivo* application of cold atmospheric plasma. *Contrib. Plasma Phys.* **54**, 104–117
26. Metelmann, H.-R., Vu, T. T., Do, H. T., Le, T. N., Hoang, T. H., Phi, T. T., Luong, T. M., Doan, V. T., Nguyen, T. T., Nguyen, T. H., Nguyen, T. L., Le, D. Q., Le, T. K., von Woedtke, T., Bussiahn, R., Weltmann, K.-D., Khalili, R., Podmelle, F., and Yacoob, S. (2013) Scar formation of laser skin lesions after cold atmospheric pressure plasma (CAP) treatment: a clinical long term observation. *Clin. Plasma Med.* **1**, 30–35
27. Jaiswal, A. K. (2004) Nrf2 signaling in coordinated activation of antioxidant gene expression. *Free Radic. Biol. Med.* **36**, 1199–1207
28. Cullinan, S. B., Gordan, J. D., Jin, J., Harper, J. W., and Diehl, J. A. (2004) The Keap1-BTB protein is an adaptor that bridges Nrf2 to a Cul3-based E3 ligase: oxidative stress sensing by a Cul3-Keap1 ligase. *Mol. Cell. Biol.* **24**, 8477–8486
29. Sun, Z., Zhang, S., Chan, J. Y., and Zhang, D. D. (2007) Keap1 controls postinduction repression of the Nrf2-mediated antioxidant response by escorting nuclear export of Nrf2. *Mol. Cell. Biol.* **27**, 6334–6349
30. Nguyen, T., Sherratt, P. J., Nioi, P., Yang, C. S., and Pickett, C. B. (2005) Nrf2 controls constitutive and inducible expression of ARE-driven genes through a dynamic pathway involving nucleocytoplasmic shuttling by Keap1. *J. Biol. Chem.* **280**, 32485–32492
31. Igarashi, K., and Sun, J. (2006) The heme-Bach1 pathway in the regulation of oxidative stress response and erythroid differentiation. *Antioxid. Redox Signal.* **8**, 107–118
32. Reichard, J. F., Sartor, M. A., and Puga, A. (2008) BACH1 is a specific repressor of HMOX1 that is inactivated by arsenite. *J. Biol. Chem.* **283**, 22363–22370
33. Oyake, T., Itoh, K., Motohashi, H., Hayashi, N., Hoshino, H., Nishizawa, M., Yamamoto, M., and Igarashi, K. (1996) Bach proteins belong to a novel family of BTB-basic leucine zipper transcription factors that interact with MafK and regulate transcription through the NF-E2 site. *Mol. Cell. Biol.* **16**, 6083–6095
34. Sun, J., Hoshino, H., Takaku, K., Nakajima, O., Muto, A., Suzuki, H., Tashiro, S., Takahashi, S., Shibahara, S., Alam, J., Taketo, M. M., Yamamoto, M., and Igarashi, K. (2002) Hemoprotein Bach1 regulates enhancer availability of heme oxygenase-1 gene. *EMBO J.* **21**, 5216–5224
35. Bekešchus, S., Masur, K., Kolata, J., Wende, K., Schmidt, A., Bundscherer, L., Barton, A., Kramer, A., Bröker, B., and Weltmann, K.-D. (2013) Human mononuclear cell survival and proliferation is modulated by cold atmospheric plasma jet. *Plasma Process. Polym.* **10**, 706–713
36. McCall, M. N., Bolstad, B. M., and Irizarry, R. A. (2010) Frozen robust multiarray analysis (fRMA). *Biostatistics* **11**, 242–253
37. Green, G. H., and Diggle, P. J. (2007) On the operational characteristics of the Benjamini and Hochberg false discovery rate procedure. *Stat. Appl. Genet. Mol. Biol.* **6**, Article27
38. Valencia, A., and Kochevar, I. E. (2008) Nox1-based NADPH oxidase is the major source of UVA-induced reactive oxygen species in human keratinocytes. *J. Invest. Dermatol.* **128**, 214–222
39. Blackert, S., Haertel, B., Wende, K., von Woedtke, T., and Lindequist, U. (2013) Influence of non-thermal atmospheric pressure plasma on cellular structures and processes in human keratinocytes (HaCaT). *J. Dermatol. Sci.* **70**, 173–181
40. Wende, K., Straßenburg, S., Haertel, B., Harms, M., Holtz, S., Barton, A., Masur, K., von Woedtke, T., and Lindequist, U. (2014) Atmospheric pressure plasma jet treatment evokes transient oxidative stress in HaCaT keratinocytes and influences cell physiology. *Cell Biol. Int.* **38**, 412–425
41. Correa-Costa, M., Azevedo, H., Amano, M. T., Gonçalves, G. M., Hyane, M. I., Cenedeze, M. A., Renesto, P. G., Pacheco-Silva, A., Moreira-Filho, C. A., and Câmara, N. O. (2012) Transcriptome analysis of renal ischemia/reperfusion injury and its modulation by ischemic pre-conditioning or hemin treatment. *PLoS One* **7**, e49569
42. Wende, K., Barton, A., Bekešchus, S., Bundscherer, L., Schmidt, A., Weltmann, K.-D., and Masur, K. (2013) Proteomic tools to characterize non-thermal plasma effects in eukaryotic cells. *Plasma Med.* **3**, 81–95
43. Emmert, S., Brehmer, F., Hänßle, H., Helmke, A., Mertens, N., Ahmed, R., Simon, D., Wandke, D., Maus-Friedrichs, W., Daeschlein, G., Schön, M. P., and Viöl, W. (2013) Atmospheric pressure plasma in dermatology: ulcer treatment and much more. *Clin. Plasma Med.* **1**, 24–29
44. Hirakawa, S., Saito, R., Ohara, H., Okuyama, R., and Aiba, S. (2011) Dual oxidase 1 induced by Th2 cytokines promotes STAT6 phosphorylation via oxidative inactivation of protein tyrosine phosphatase 1B in human epidermal keratinocytes. *J. Immunol.* **186**, 4762–4770
45. Loo, A. E., Wong, Y. T., Ho, R., Wasser, M., Du, T., Ng, W. T., and Halliwell, B. (2012) Effects of hydrogen peroxide on wound healing in mice in relation to oxidative damage. *PLoS One* **7**, e49215
46. Reuter, S., Tresp, H., Wende, K., Hammer, M. U., Winter, J., Masur, K., Schmidt-Bleker, A., and Weltmann, K.-D. (2012) From RONS to ROS: tailoring plasma jet treatment of skin cells. *Plasma Sci. IEEE Trans.* **40**, 2986–2993
47. Winter, J., Wende, K., Masur, K., Iseni, S., Dünnbier, M., Hammer, M. U., Tresp, H., Weltmann, K.-D., and Reuter, S. (2014) Feed gas humidity: a vital parameter affecting a cold atmospheric-pressure plasma jet and plasma-treated human skin cells. *J. Phys. D Appl. Phys.* **46**, 295401
48. Kaushik, A. K., Vareded, S. K., Basu, S., Putluri, V., Putluri, N., Panzitt, K., Brennan, C. A., Chinnaiyan, A. M., Vergara, I. A., Erho, N., Weigel, N. L., Mitsiades, N., Shojaie, A., Palapattu, G., Michailidis, G., and Sreekumar, A. (2014) Metabolomic profiling identifies biochemical pathways associated with castration-resistant prostate cancer. *J. Proteome Res.* **13**, 1088–1100
49. Barton, A., Wende, K., Bundscherer, L., Hasse, S., Schmidt, A., Bekešchus, S., Weltmann, K.-D., Lindequist, U., and Masur, K. (2013) Non-thermal plasma increases expression of wound healing related genes in a keratinocyte cell line. *Plasma Med.* **3**, 125–136
50. Bundscherer, L., Wende, K., Ottmüller, K., Barton, A., Schmidt, A., Bekešchus, S., Hasse, S., Weltmann, K. D., Masur, K., and Lindequist, U. (2013) Impact of non-thermal plasma treatment on MAPK signaling pathways of human immune cell lines. *Immunobiology* **218**, 1248–1255
51. Haertel, B., Hähnel, M., Blackert, S., Wende, K., von Woedtke, T., and Lindequist, U. (2012) Surface molecules on HaCaT keratinocytes after interaction with non-thermal atmospheric pressure plasma. *Cell Biol. Int.* **36**, 1217–1222
52. Arndt, S., Unger, P., Wacker, E., Shimizu, T., Heinlin, J., Li, Y. F., Thomas, H. M., Morfill, G. E., Zimmermann, J. L., Bosserhoff, A. K., and Karrer, S. (2013) Cold atmospheric plasma (CAP) changes gene expression of key molecules of the wound healing machinery and improves wound healing *in vitro* and *in vivo*. *PLoS One* **8**, e79325
53. Haertel, B., Volkmann, F., von Woedtke, T., and Lindequist, U. (2012) Differential sensitivity of lymphocyte subpopulations to non-thermal atmospheric-pressure plasma. *Immunobiology* **217**, 628–633
54. Lichtenfels, R., Mouggiakakos, D., Johansson, C. C., Dressler, S. P., Recktenwald, C. V., Kiessling, R., and Seliger, B. (2012) Comparative expression profiling of distinct T cell subsets undergoing oxidative stress. *PLoS One* **7**, e41345
55. Winter, J., Tresp, H., Hammer, M., Iseni, S., Kupsch, S., Schmidt-Bleker, A., Wende, K., Dünnbier, M., Masur, K., Weltmann, K.-D., and Reuter, S. (2014) Tracking plasma generated H<sub>2</sub>O<sub>2</sub> from gas into liquid phase and revealing its dominant impact on human skin cells. *J. Phys. D Appl. Phys.* **47**, 285401
56. Lukes, P., Dolezalova, E., Sisrova, I., and Clupek, M. (2014) Aqueous-phase chemistry and bactericidal effects from an air discharge plasma in contact with water: evidence for the formation of peroxyxynitrite through a pseudo-second-order post-discharge reaction of H<sub>2</sub>O<sub>2</sub> and HNO<sub>2</sub>. *Plasma Sources Sci. Technol.* **23**, 015019
57. Nguyen, T., Nioi, P., and Pickett, C. B. (2009) The Nrf2-antioxidant response element signaling pathway and its activation by oxidative stress. *J. Biol. Chem.* **284**, 13291–13295
58. Christman, S. A., Kong, B. W., Landry, M. M., Kim, H., and Foster, D. N. (2005) Modulation of p53 expression and its role in the conversion to a fully immortalized chicken embryo fibroblast line. *FEBS Lett.* **579**, 6705–6715
59. Pekovic-Vaughan, V., Gibbs, J., Yoshitane, H., Yang, N., Pathirana, D., Guo, B., Sagami, A., Taguchi, K., Bechtold, D., Loudon, A., Yamamoto, M., Chan, J., van der Horst, G. T., Fukada, Y., and Meng, Q. J. (2014) The circadian clock regulates rhythmic activation of the NRF2/glutathione-mediated antioxidant defense pathway to modulate pulmonary fibrosis. *Genes Dev.* **28**, 548–560

60. Huang, B. W., Ray, P. D., Iwasaki, K., and Tsuji, Y. (2013) Transcriptional regulation of the human ferritin gene by coordinated regulation of Nrf2 and protein arginine methyltransferases PRMT1 and PRMT4. *FASEB J.* **27**, 3763–3774
61. Zhao, R., Hou, Y., Zhang, Q., Woods, C. G., Xue, P., Fu, J., Yarborough, K., Guan, D., Andersen, M. E., and Pi, J. (2012) Cross-regulations among NRFs and KEAP1 and effects of their silencing on arsenic-induced antioxidant response and cytotoxicity in human keratinocytes. *Environ. Health Perspect.* **120**, 583–589
62. Siegel, D., Anwar, A., Winski, S. L., Kepa, J. K., Zolman, K. L., and Ross, D. (2001) Rapid polyubiquitination and proteasomal degradation of a mutant form of NAD(P)H: quinone oxidoreductase 1. *Mol. Pharmacol.* **59**, 263–268
63. Pham, R. T., Gardner, J. L., and Gallagher, E. P. (2002). Conjugation of 4-hydroxynonenal by largemouth bass (*Micropterus salmoides*) glutathione S-transferases. *Mar. Environ. Res.* **54**, 291–295
64. Roman, M., Jitaru, P., and Barbante, C. (2014) Selenium biochemistry and its role for human health. *Metallomics* **6**, 25–54
65. Deleted in proof
66. Jazwa, A., Loboda, A., Golda, S., Cisowski, J., Szlag, M., Zagorska, A., Sroczyńska, P., Drukala, J., Jozkowicz, A., and Dulak, J. (2006) Effect of heme and heme oxygenase-1 on vascular endothelial growth factor synthesis and angiogenic potency of human keratinocytes. *Free Radic. Biol. Med.* **40**, 1250–1263
67. Itoh, K., Mochizuki, M., Ishii, Y., Ishii, T., Shibata, T., Kawamoto, Y., Kelly, V., Sekizawa, K., Uchida, K., and Yamamoto, M. (2004) Transcription factor Nrf2 regulates inflammation by mediating the effect of 15-deoxy- $\Delta(12,14)$ -prostaglandin J<sub>2</sub>. *Mol. Cell. Biol.* **24**, 36–45
68. Wagener, F. A., Scharstuhl, A., Tyrrell, R. M., Von den Hoff, J. W., Jozkowicz, A., Dulak, J., Russel, F. G., and Kuijpers-Jagtman, A. M. (2010) The heme-heme oxygenase system in wound healing; implications for scar formation. *Curr. Drug Targets* **11**, 1571–1585
69. Grochot-Przeczek, A., Kotlinowski, J., Kozakowska, M., Starowicz, K., Jagodzinska, J., Stachurska, A., Volger, O. L., Bukowska-Strakova, K., Florczyk, U., Tertel, M., Jazwa, A., Szade, K., Stepniewski, J., Loboda, A., Horrevoets, A. J., Dulak, J., and Jozkowicz, A. (2014) Heme oxygenase-1 is required for angiogenic function of bone marrow-derived progenitor cells: role in therapeutic revascularization. *Antioxid. Redox Signal.* **20**, 1677–1692
70. Frank, S., Hübner, G., Breier, G., Longaker, M. T., Greenhalgh, D. G., and Werner, S. (1995) Regulation of vascular endothelial growth factor expression in cultured keratinocytes. Implications for normal and impaired wound healing. *J. Biol. Chem.* **270**, 12607–12613
71. Dulak, J., Józkowicz, A., Foresti, R., Kasza, A., Frick, M., Huk, I., Green, C. J., Pachinger, O., Weidinger, F., and Motterlini, R. (2002) Heme oxygenase activity modulates vascular endothelial growth factor synthesis in vascular smooth muscle cells. *Antioxid. Redox Signal.* **4**, 229–240
72. Calkins, M. J., Jakel, R. J., Johnson, D. A., Chan, K., Kan, Y. W., and Johnson, J. A. (2005) Protection from mitochondrial complex II inhibition in vitro and in vivo by Nrf2-mediated transcription. *Proc. Natl. Acad. Sci. U.S.A.* **102**, 244–249
73. Hirota, A., Kawachi, Y., Itoh, K., Nakamura, Y., Xu, X., Banno, T., Takahashi, T., Yamamoto, M., and Otsuka, F. (2005) Ultraviolet A irradiation induces NF-E2-related factor 2 activation in dermal fibroblasts: protective role in UVA-induced apoptosis. *J. Invest. Dermatol.* **124**, 825–832
74. Itoh, K., Wakabayashi, N., Katoh, Y., Ishii, T., O'Connor, T., Yamamoto, M. (2003) Keap1 regulates both cytoplasmic-nuclear shuttling and degradation of Nrf2 in response to electrophiles. *Genes Cells* **8**, 379–391
75. Suzuki, H., Tashiro, S., Sun, J., Doi, H., Satomi, S., and Igarashi, K. (2003) Cadmium induces nuclear export of Bach1, a transcriptional repressor of heme oxygenase-1 gene. *J. Biol. Chem.* **278**, 49246–49253
76. Ishikawa, M., Numazawa, S., and Yoshida, T. (2005) Redox regulation of the transcriptional repressor Bach1. *Free Radic. Biol. Med.* **38**, 1344–1352
77. Barrientos, S., Stojadinovic, O., Golinko, M. S., Brem, H., and Tomic-Canic, M. (2008) Growth factors and cytokines in wound healing. *Wound Repair Regen.* **16**, 585–601
78. Kayahara, M., Wang, X., and Tournier, C. (2005) Selective regulation of c-jun gene expression by mitogen-activated protein kinases via the 12-O-tetradecanoylphorbol-13-acetate-responsive element and myocyte enhancer factor 2 binding sites. *Mol. Cell. Biol.* **25**, 3784–3792
79. Cargnello, M., and Roux, P. P. (2011) Activation and function of the MAPKs and their substrates, the MAPK-activated protein kinases. *Microbiol. Mol. Biol. Rev.* **75**, 50–83
80. Antico Arciuch, V. G., Elguero, M. E., Poderoso, J. J., and Carreras, M. C. (2012) Mitochondrial regulation of cell cycle and proliferation. *Antioxid. Redox Signal.* **16**, 1150–1180
81. Jurzak, M., and Adamczyk, K. (2013) Influence of genistein on c-Jun, c-Fos and Fos-B of AP-1 subunits expression in skin keratinocytes, fibroblasts and keloid fibroblasts cultured in vitro. *Acta Pol. Pharm.* **70**, 205–213
82. Vesely, P. W., Staber, P. B., Hoefler, G., and Kenner, L. (2009) Translational regulation mechanisms of AP-1 proteins. *Mutat. Res.* **682**, 7–12
83. Behmoaras, J., Bhargal, G., Smith, J., McDonald, K., Mutch, B., Lai, P. C., Domin, J., Game, L., Salama, A., Foxwell, B. M., Pusey, C. D., Cook, H. T., and Aitman, T. J. (2008) Jund is a determinant of macrophage activation and is associated with glomerulonephritis susceptibility. *Nat. Genet.* **40**, 553–559
84. Mann, A., Breuhahn, K., Schirmacher, P., and Blessing, M. (2001) Keratinocyte-derived granulocyte-macrophage colony stimulating factor accelerates wound healing: stimulation of keratinocyte proliferation, granulation tissue formation, and vascularization. *J. Invest. Dermatol.* **117**, 1382–1390
85. Trachootham, D., Lu, W., Ogasawara, M. A., Nilsa, R. D., and Huang, P. (2008) Redox regulation of cell survival. *Antioxid. Redox Signal.* **10**, 1343–1374
86. Sporn, M. B., and Liby, K. T. (2012) NRF2 and cancer: the good, the bad and the importance of context. *Nat. Rev. Cancer* **12**, 564–571
87. Shibata, T., Kokubu, A., Gotoh, M., Ojima, H., Ohta, T., Yamamoto, M., and Hirohashi, S. (2008) Genetic alteration of Keap1 confers constitutive Nrf2 activation and resistance to chemotherapy in gallbladder cancer. *Gastroenterology* **135**, 1358–1368, 1368.e1–4
88. Boxhammer, V., Li, Y. F., Köritzer, J., Shimizu, T., Maisch, T., Thomas, H. M., Schlegel, J., Morfill, G. E., and Zimmermann, J. L. (2013) Investigation of the mutagenic potential of cold atmospheric plasma at bactericidal dosages. *Mutat. Res.* **753**, 23–28